Smc5/6 silences episomal transcription by a three-step function

Abdul, Fabien; Diman, Aurélie; Baechler, Bastien; Ramakrishnan, Dhivya; Kornyeyev, Dmytro; Beran, Rudolf K.; Fletcher, Simon P.; Strubin, Michel

How to cite

ABDUL, Fabien et al. Smc5/6 silences episomal transcription by a three-step function. In: Nature structural & molecular biology, 2022. doi: 10.1038/s41594-022-00829-0

This publication URL: https://archive-ouverte.unige.ch/unige:163380
Publication DOI: 10.1038/s41594-022-00829-0

1. Extended Data

Figure #	Figure title One sentence only	Filename This should be the name the file is saved as when it is uploaded to our system. Please include the file extension. i.e.: *Smith_ED_Fig1.jpg*	Figure Legend If you are citing a reference for the first time in these legends, please include all new references in the main text Methods References section, and carry on the numbering from the main References section of the paper. If your paper does not have a Methods section, include all new references at the end of the main Reference list.
Extended Data Fig. 1	**Smc5/6 is the only SMC complex to silence expression of the episomal HBV genome. Related to Figure 1.**	NSMB-A45419_ED1.TIF	**a,** PHH were transfected with a non-targeting control siRNA (siCtrl) or with siRNA targeting the indicated Smc subunits. Cells were then incubated for 3 days and infected with wild-type (WT) or an HBx-deficient (ΔX) HBV. HBeAg secretion, a marker for HBV gene expression, was measured 14 days later. HBeAg levels are expressed as a percentage of those in control cells infected with HBV(WT) (grey bars) or in siSmc6-treated cells infected with HBV(ΔX) (black bars). Data are means ± SEM of three independent experiments with samples from one PHH donor. The schematic diagram summarizing the design of the study is shown at the top. **b,** The mRNA levels of the indicated Smc proteins in the samples analyzed in **a** were determined by real-time RT–PCR and normalized to β-actin. Values are expressed as a percentage of those in control cells (siCtrl). Data are means ± SEM of three independent experiments with one PHH donor. **c,** Luciferase assay for the ChIP experiment presented in Fig, 1c. Data are means ± SEM of 2 independent experiments. **d,** HA-Smc2 assembles into a condensin complex. Whole extracts prepared from HepG2 cells expressing the indicated HA-tagged SMC protein in a CRISPR/Cas9 knockout background were immunoprecipitated with anti-HA antibodies. The amounts recovered and the presence of Smc5, CAP-H and Nse4 in the eluates were assessed by Western blotting. CAP-H and Nse4 are the kleisin subunits of, respectively, condensin (Smc2) and the Smc5/6 complex. See Fig. 1a. Actin serves as a negative control. The experiment was repeated twice independently with similar results.
Extended Data Fig. 2	**Effect of single-subunit depletion on Smc5/6 complex integrity and restriction activity**	NSMB-A45419_ED2.TIF	HepG2 cells were transduced with lentiviral constructs expressing Cas9 alone (Ctrl) or Cas9 together with sgRNA targeting the indicated Smc5/6 subunits, or with lentiviruses encoding GFP or GFP-HBx, as indicated. After selection, cells were transfected with a luciferase reporter plasmid. Luciferase assay and Western blot analysis were performed 5 days later. Hsp90 serves as a loading control. Unessential lanes were removed from the original blot images. Luciferase activity is relative to that measured

			in cells expressing HBx, which was set to 10. Data are means ± SEM of 3 independent experiments.
Extended Data Fig. 3	**Involvement of Smc5 and Smc6 ATP binding and hydrolysis in Smc5/6 episomal DNA binding and restriction, and degradation by HBx. Related to Figure 2.**	NSMB-A45419_ED3.TIF	**a,** Luciferase assay for the ChIP experiment presented in Fig. 2c. Data are means ± SEM of 3 independent experiments. **b,** Smc6 ATP binding mutants normally assemble into Smc5/6 complexes. Whole extracts prepared from HepG2 cells depleted of Smc6 and expressing HA-GFP or the indicated HA-tagged SMC protein were immunoprecipitated with anti-HA antibodies. The amounts recovered and the presence of other Smc5/6 subunits in the eluates were assessed by Western blotting. Hsp90 serves as a negative control. The experiment was repeated twice independently with similar results. **c,** Luciferase assay for the ChIP experiment presented in Fig, 2d. Data are means ± SEM of 3 independent experiments. **d,** HepG2 cells depleted of Smc6 and expressing GFP or the indicated wild-type or mutant Smc6 proteins from lentiviral vectors exactly as in Fig. 2b were also transduced with GFP or GFP-HBx. Western blot analysis was performed as before. GAPDH serves as a loading control. The experiment was repeated thrice independently with similar results.
Extended Data Fig. 4	**Nse4a performs an essential function in Smc5/6 restriction for which Nse4b cannot substitute. Related to Figure 3.**	NSMB-A45419_ED4.TIF	**a,** Schematic diagram of Nse4a (long), the shorter isoform of Nse4a, Nse4b and the Nse4b variant bearing the N-terminal region unique to Nse4a. White boxes indicate Nse4a sequences and the region of the short Nse4a protein common to both splicing isoforms. Hatched boxes indicate regions of Nse4b showing homology to Nse4a. The grey box indicates a region with no homology. Highlighted in black are the highly conserved N-terminal and C-terminal kleisin domains that have the potential to form helix-turn-helix and winged-helix motifs and are involved in Nse4 interaction with Smc6 and Smc5, respectively (Palecek et al., 2006; Vondrova et al., 2020). **b,** Luciferase assay for the ChIP experiment presented in Fig. 3b. Data are means ± SEM of 2 independent experiments. **c,** Same experiment as in Fig. 3a but including an Nse4b chimeric protein carrying the N-terminal region unique to Nse4a (Nse4a-b; see panel **a**). Expression of Nse4b and Nse4a-b was inferred from their stabilization effect on the other Smc5/6 subunits (lane 8). Data are means ± SEM of 2 independent experiments.
Extended Data Fig. 5	**Nse1 and Nse3 DNA-binding mutants are functional in vivo.**	NSMB-A45419_ED5.TIF	**a,b,** Control HepG2 cells (black bars) and cells depleted of Nse1 (**a**) or Nse3 (**b**; grey bars) were transfected with a luciferase reporter plasmid and shortly after transduced with GFP or the corresponding wild-type or DNA-binding

			mutant protein as indicated (Zabrady et al., 2016). Luciferase assay and Western blot analysis were as before. Data are means ± SEM of 3 independent experiments.
Extended Data Fig. 6	**HBx triggers Smc5/6 degradation in the absence of Nse2. Related to Figure 4.**	NSMB-A45419_ED6.TIF	**Extended Data Figure 6. HBx triggers Smc5/6 degradation in the absence of Nse2. Related to Figure 4.** **a,** Control HepG2 cells (black bars) and cells depleted of Nse2 (grey bars) were transfected with a reporter gene and transduced with GFP or Flag-tagged Nse2 (F-Nse2). Cells were then split and further transduced with GFP or GFP-HBx. Luciferase assay and Western blot analysis were as before. Data are expressed as mean ± SEM of 2 independent experiments. **b,** Luciferase assay for the ChIP experiment presented in Fig. 4b. Data are expressed as mean ± SEM of 3 independent experiments. **c,** Single channel confocal images of middle right panels merged images presented in Fig. 4d.
Extended Data Fig. 7	**HBx triggers Smc5/6 degradation in the absence of SLF2. Related to Figure 5.**	NSMB-A45419_ED7.TIF	**a,** Control HepG2 cells (black bars) and cells depleted of SLF2 (grey bars) were transfected with a reporter gene and shortly after transduced with GFP, GFP-HBx and/or SLF2 in the indicated combinations. Luciferase assay and Western blot analysis were performed as before. Data are expressed as mean ± SEM of 2 independent experiments. **b,** Luciferase assay for the ChIP experiment presented in Fig. 5b. Data are means ± SEM of 2 independent experiments. **c,** Single channel confocal images of middle right panels merged images presented in Fig. 5d. **d,** Luciferase assay for the ChIP experiment presented in Fig. 5e. Data are means ± SEM of 4 independent experiments.

2. Supplementary Information:

A. Flat Files

Item	Present?	Filename This should be the name the file is saved as when it is uploaded to our system, and should include the file extension. The extension must be .pdf	A brief, numerical description of file contents. i.e.: *Supplementary Figures 1-4, Supplementary Discussion, and Supplementary Tables 1-4.*
Reporting Summary	Yes	NSMB-A45419-	

		nr-reporting-summary FINAL.pdf
Peer Review Information	Yes	*TPRFile_Strubin.pdf*

B. Additional Supplementary Files

Type	Number If there are multiple files of the same type this should be the numerical indicator. i.e. "1" for Video 1, "2" for Video 2, etc.	Filename This should be the name the file is saved as when it is uploaded to our system, and should include the file extension. i.e.: *Smith_ Supplementary_Video_1.mov*	Legend or Descriptive Caption Describe the contents of the file
Supplementary Table	1	Suplementary tables.pdf	*Supplementary Tables 1-3*

3. Source Data

Parent Figure or Table	Filename This should be the name the file is saved as when it is uploaded to our system, and should include the file extension. i.e.: *Smith_SourceData_Fig1.xls,* or *Smith_ Unmodified_Gels_Fig1.pdf*	Data description i.e.: Unprocessed Western Blots and/or gels, Statistical Source Data, etc.
All figures	NSMB-A45419_Source_Data_fullscan.pptx	Unprocessed Western Blots
Figure 1	NSMB-A45419_Figure_1.xlsx	Source Data of graphical representations used in figure 1
Figure 2	NSMB-A45419_Figure_2.xlsx	Source Data of graphical representations used in figure 2
Figure 3	NSMB-A45419_Figure_3.xlsx	Source Data of graphical representations used in figure 3
Figure 4	NSMB-A45419_Figure_4.xlsx	Source Data of graphical representations used in figure 4
Figure 5	NSMB-A45419_Figure_5.xlsx	Source Data of graphical representations used in figure 5
Extended Data Figure 1	NSMB-A45419_Extended_Data_Figure_1.xlsx	Source Data of graphical representations used in extended figure 1
Extended Data Figure 2	NSMB-A45419_Extended_Data_Figure_2.xlsx	Source Data of graphical representations used in extended figure 2
Extended Data Figure 3	NSMB-A45419_Extended_Data_Figure_3.xlsx	Source Data of graphical representations used in extended figure 3
Extended Data Figure 4	NSMB-A45419_Extended_Data_Figure_4.xlsx	Source Data of graphical representations used in extended figure 4
Extended Data Figure 5	NSMB-A45419_Extended_Data_Figure_5.xlsx	Source Data of graphical representations used in extended figure 5
Extended Data Figure 6	NSMB-A45419_Extended_Data_Figure_6.xlsx	Source Data of graphical representations used in extended figure 6
Extended Data Figure 7	NSMB-A45419_Extended_Data_Figure_7.xlsx	Source Data of graphical representations used in extended figure 7

Smc5/6 silences episomal transcription by a three-step function

Fabien Abdul[1], Aurélie Diman[1], Bastien Baechler[1], Dhivya Ramakrishnan[2], Dmytro Kornyeyev[2], Rudolf K. Beran[2], Simon P. Fletcher[2], and Michel Strubin[1]*

[1] Department of Microbiology and Molecular Medicine, University Medical Centre (C.M.U.), 1211 Geneva 4, Switzerland

[2] Gilead Sciences, Foster City, California, USA

* Corresponding author: *Tel*: (41-22) 379 5690

Fax: (41-22) 379 5702

E-mail: Michel.Strubin@unige.ch

Abstract

In addition to its role in chromosome maintenance, the six-member Smc5/6 complex functions as a restriction factor that binds to and transcriptionally silences viral and other episomal DNA. However, the underlying mechanism is unknown. Here we show that transcriptional silencing by the human Smc5/6 complex is a three-step process. The first step is entrapment of the episomal DNA by a mechanism dependent on Smc5/6 ATPase activity and a function of its Nse4a subunit for which the Nse4b paralog cannot substitute. The second step results in Smc5/6 recruitment to PML nuclear bodies by SLF2 (human ortholog of Nse6). The third step promotes silencing through a mechanism requiring Nse2 but not its SUMO ligase activity. In contrast, the related cohesin and condensin complexes fail to bind to and silence episomal DNA, thus pointing to a property unique to Smc5/6.

Introduction

The Smc5/6 complex is one of three structurally and functionally related Structural Maintenance of Chromosomes (SMC) complexes that have been identified in eukaryotes. These ring-shaped complexes associate with chromosomal DNA through topological entrapment to play distinct and essential roles in chromosome organization and in maintaining genomic stability [1]. They include condensin, which contains the Smc2 and Smc4 core subunits and mediates chromosome condensation during mitosis, cohesin, which contains Smc1 and Smc3 and holds newly replicated sister chromatids together to ensure their faithful segregation, and the Smc5/6 complex, whose functions remain unclear [1]. As with the other SMC complexes, the backbone of Smc5/6 is formed by a heterodimer of the two Smc proteins, Smc5 and Smc6 (Fig. 1a) [2]. Each protein contains a central hinge region flanked by two long α-helical arms that fold back on each other forming a coiled-coil structure, thereby bringing the globular N- and C-termini together to form the so-called head domain that has ATPase activity. The two proteins interact via their hinge domain [3], thus forming a V-shaped structure, and associate with four non-SMC proteins (Nse), designated Nse1 to Nse4 [4,5]. Nse2 has SUMOylation activity and binds the coiled-coil domain of Smc5, whereas Nse4 forms a heterotrimer with Nse1 and Nse3 and bridges the globular head domains of Smc5 and Smc6 to form a ring-like structure large enough to encircle two DNA molecules [6].

The Smc5/6 complex is essential and conserved from yeast to humans and has been attributed a number of functions [7–9]. One is to assist repair of double strand-breaks (DSBs) [10,11]. Another is to prevent incomplete replication by rescuing stalled replication forks [12–14]. Both pathways involve homologous recombination between sister chromatids and, if unsuccessful, can lead to genomic instability [7,8,15]. Smc5/6 is thought to prevent this by inhibiting formation or promoting removal of toxic recombination intermediates [14,16]. Additionally, Smc5/6 has non-repair functions [17]. Specifically, it has been proposed to facilitate replication elongation by

binding to and stabilizing sister-chromatid intertwines that accumulate behind the advancing replication fork, thereby relieving the topological tension generated [18,19].

Recent work revealed that in addition to its essential roles in chromosome maintenance, Smc5/6 also functions as a host restriction factor against hepatitis B virus (HBV) [20,21]. Specifically, Smc5/6 binds to the circular HBV DNA genome, thereby blocking viral transcription [20]. HBV antagonizes this restriction by expressing the regulatory HBx protein, which targets Smc5/6 for proteasomal degradation through its recruitment to the cellular DDB1-containing E3 ubiquitin ligase [20–22]. Restriction by Smc5/6 is conserved in mammals [23] and is not limited to the HBV genome. Expression of any reporter construct is silenced by Smc5/6, and thus stimulated by HBx expression or by Smc5/6 depletion, regardless of the enhancer and promoter type [20,24]. However, this occurs only if the DNA remains extrachromosomal. Thus, Smc5/6 functions as a broadly acting restriction factor that operates selectively on extrachromosomal (i.e. episomal) DNA templates to silence HBV and potentially other clinically important DNA viruses [25,26]. How Smc5/6 detects and binds preferentially to episomal DNA and how it restricts gene transcription remains elusive.

As a first step towards addressing these questions, we performed a structure-function analysis of Smc5/6 to identify enzymatic activities and structural properties implicated in its restriction function. Specifically, we tested individual Smc5/6 subunit mutants and/or naturally occurring isoforms for their ability to promote episomal silencing using a functional complementation assay. We also explored whether the other members of the SMC family, cohesin and condensin, exhibit similar restriction activities. Our results reveal that episomal restriction is unique to Smc5/6. They further show that silencing is a three-step process that includes Smc5/6 binding to DNA, recruitment to promyelocytic leukemia nuclear bodies (PML-NBs) by SLF2, and silencing by a mechanism that implicates a novel function of Nse2. They also

92 provide new information about how and under which circumstances the HBx protein interacts
93 with Smc5/6, an issue that may have therapeutic implications.

94

95

Results

Smc5/6 binds and transcriptionally silences episomal DNA

As a first step towards determining the requirements for Smc5/6 binding to and/or restriction of episomal DNA, we examined whether the other members of the SMC family, cohesin and condensin, would exhibit similar properties (Fig. 1a). We inactivated the three SMC complexes in HepG2 cells using CRISPR/Cas9 and monitored the consequence on episomal gene expression. While depletion of Smc6 led to a strong increase in activity of a transiently transfected luciferase reporter, as expected [20], depletion of Smc2 (condensin) or Smc3 (cohesin) had no such effect (Fig. 1b). In line with this finding, siRNA-mediated knockdown of cohesin or condensin also had no effect on viral antigen production from wild-type or HBx-negative HBV in primary human hepatocytes (PHH), in which efficient HBV transcription relies on Smc5/6 degradation by HBx (Extended Data Fig. 1a,b) [20,21]. To examine if this lack of effect was due to cohesin and/or condensin failing to bind episomal DNA, we performed chromatin immunoprecipitation (ChIP) using knockout cells complemented with HA-epitope tagged versions of the corresponding SMC subunits. We confirmed that Smc5/6 binds to the episomal reporters (Fig. 1c and Extended Data Fig. 1c) [20]. In contrast, cohesin did not bind episomal DNA, despite showing strong binding at chromosomal locations where the complex has been reported to associate [27] (Fig. 1c; see Supplementary Table 3). On the other hand, no signal for condensin was detected at any region examined [28], including episomal DNA, under conditions where condensin complexes containing HA-tagged Smc2 were readily detected (Fig. 1c and Extended Data Fig. 1d). Hence, binding and silencing of episomal DNA templates is unique to Smc5/6 and not a general property of the SMC complexes.

ATP binding and hydrolysis are required for restriction

120 Consistent with previous studies [20,29], we found that depletion of any Smc5/6 subunit other
121 than Nse2 results in complex disruption by degradation of the other components, and thus in
122 loss of restriction activity (Extended Data Fig. 2). We tested individual Smc5/6 subunit
123 mutants and naturally occurring isoforms for both complex formation and functional
124 complementation in a CRISPR/Cas9-knockout background.

125 The N-terminal and C-terminal parts of SMC proteins fold into a globular "head domain" that
126 contains ATP binding and hydrolysis motifs (Fig. 1a) [30]. To examine the role of ATP binding
127 and ATP hydrolysis in Scm5/6-mediated episomal restriction, we engineered Smc5 and Smc6
128 point mutations predicted to abolish either ATP binding or ATP hydrolysis [30–32]. The mutants
129 were expressed in HepG2 cells depleted for the corresponding endogenous protein and tested
130 for their ability to restore stable complex formation and restrict transcription of an episomal
131 luciferase reporter construct. Figure 2 shows that depletion of Smc5 resulted in decreased
132 Smc5 and Nse4 protein levels and concomitant increase in reporter gene activity (Fig. 2a,
133 lanes 1 and 6). Complementation with wild-type Smc5 restored normal Nse4 protein levels,
134 indicating stable Smc5/6 complex formation, and reestablished silencing. (Fig. 2a, lanes 6 and
135 7). By contrast, and despite having comparable stabilizing effects on Nse4, the two Smc5
136 ATP binding mutants tested, K86E and D1019A, did not rescue silencing, neither did the
137 ATP hydrolysis mutant E1020A (Fig. 2a, lanes 8-10). The same results were obtained when
138 equivalent mutations were introduced into Smc6 (Fig. 2b). Thus, both ATP binding and ATP
139 hydrolysis activities of Smc5 and Smc6 are required for episomal silencing.

140 To determine if the lack of restriction activity of the Smc5- and Smc6-mutant complexes
141 reflects a failure to associate with episomal DNA, we performed ChIP experiments. For this,
142 we engineered Smc6-depleted HepG2 cells to express HA-tagged versions of the wild-type or
143 Smc6 mutants. As anticipated, wild-type HA-Smc6 showed strong binding to the episomal
144 luciferase reporter but not to the chromosomal actin gene (Fig. 2c and Extended Data Fig. 3a)

[20]. Binding was markedly reduced upon co-expression of HBx, consistent with the HA-tagged Smc6 protein functioning as a subunit of Smc5/6 (Fig. 2c, lanes 2 and 5). By contrast, no signal above background was detected at either site with Smc6 ATP binding mutants, despite them being as effective as wild-type in forming Smc5/6 complexes (Fig. 2c and Extended Data Fig. 3a,b). Although being fully defective for restriction, a Smc5/6 ATP hydrolysis mutant (E1016Q) still associated with the episomal DNA template (Fig. 2d). However, this mutant reproducibly showed lower binding signals compared to wild-type Smc5/6 (Fig. 2d and Extended Data Fig. 3c), suggesting that productive association of Smc5/6 to episomal DNA involves both ATP binding and hydrolysis.

Interestingly, HBx degraded wild-type, ATP binding- and ATP hydrolysis-deficient Smc5/6 complexes with comparable efficiencies (Extended Data Fig. 3d). This indicates that HBx can bind and target the complex for destruction independently of its ATP-binding status and association to episomal DNA.

Nse4b cannot substitute for Nse4a in episomal silencing

The kleisin subunit Nse4 forms a trimer with Nse1 and Nse3 and connects the globular head domains of Smc5 and Smc6, thus completing the ring-like structure (Fig. 1a) [4,5]. Mammals have two Nse4 paralogs, Nse4a and Nse4b, which share two highly conserved kleisin domains and show approximately 50% overall identity (Extended Data Fig. 4a) [29,33,34]. Both proteins can incorporate into a Smc5/6 complex but only Nse4a was recovered in HBx pull-down experiments [20,29,34]. Consistent with a central role of Nse4 in Smc5/6 formation, CRISPR/Cas9-mediated depletion of Nse4a resulted in degradation of the remaining Smc5/6 subunits and consequent loss of episomal silencing (Fig. 3a, lanes 1 and 5). Ectopic expression of Nse4a or Nse4b in this knockout background revealed that the two proteins are equally efficient at supporting assembly of a full Smc5/6 complex (Fig. 3a). However, only the Nse4a-containing Smc5/6 exhibited episomal restriction activity. The Nse4b complex did

not (Fig. 3a), and this was due to a failure of the complex to associate with episomal DNA (Fig. 3b and Extended Data Fig. 4b). An Nse4b hybrid protein carrying the N-terminal tail unique to Nse4a was also functionally inactive (Extended Data Fig. 4a,c). Thus, Nse4b can substitute for Nse4a in Smc5/6 but the resulting complex fails to bind to and restrict episomal DNA. As was the case with the ATP-binding and ATP-hydrolysis Smc5/6 mutants, HBx efficiently triggered degradation of the Nse4b-containing Smc5/6 (Fig. 3b). This confirms that HBx-mediated degradation does not require Smc5/6 binding to episomal DNA. Given the relatively low sequence identity between Nse4a and Nse4b, it also suggests that Nse4a does not interact directly with HBx.

The Nse4a mRNA can be spliced to produce a shorter isoform of the protein that lacks the C-terminal 104 amino acids implicated in the interaction of Nse4 with Smc5 [5] (Extended Data Fig. 4a). This shorter Nse4a variant stabilized Nse1 and Nse3 but not Smc5 and Smc6, indicating formation of a stable Nse1/Nse3/Nse4 sub-complex (Fig. 3a and Extended Data Fig. 4a) [34,35]. However, the resulting sub-complex failed to promote restriction (Fig. 3a), suggesting that transcriptional silencing requires a fully assembled complex that includes Smc5 and Smc6.

Intriguingly, although ineffective for restriction, Nse4b could substitute, at least partially, for Nse4a in sustaining cell proliferation in a colony formation assay (Fig. 3c) [36]. This suggests that Nse4a and Nse4b share a common ability to support the essential cellular functions of Smc5/6 and that Nse4a has further acquired an activity uniquely required for Smc5/6 binding to episomal DNA for which Nse4b cannot substitute.

Nse1 and Nse3 DNA-binding mutants are functional in vivo

Smc5/6 loading onto chromosomes is thought to involve the interaction of the Nse1/3/4 sub-complex with DNA, with all three subunits contributing to binding [37,38]. This is supported by

194 the observation that charge reversal mutations of conserved basic residues in Nse1 and Nse3
195 reduce binding of the Nse1/3/4 sub-complex to DNA *in vitro* and are lethal when introduced
196 into *S. pombe* [38]. We tested two such mutants, Nse1(K139E) and Nse3(R229E), for episomal
197 silencing using a CRISPR/Cas9-based complementation assay and found that they retain
198 restriction activity (Extended Data Fig. 5). This raises the possibility that Smc5/6 binding to
199 chromosomal or episomal DNA may have different requirements.

200 ***Nse2 is implicated in Smc5/6 restriction but not DNA binding***

201 Nse2 is a subunit of Smc5/6 for which no functional equivalent exists in the other SMC
202 complexes. Nse2 binds the coiled-coil domain of Smc5 and possesses SUMO E3-ligase
203 activity that is conserved from yeast to human [39–41]. Nse2 sumoylates a number of cellular
204 factors involved in diverse chromosome transactions, including components of the replication
205 fork and of cohesin and condensin, as well as subunits of Smc5/6 itself [40]. Although not
206 essential for viability in mice [42], the SUMO E3 ligase activity of Nse2 has been linked to most
207 Smc5/6 cellular functions [19,43–46]. Therefore, since SUMOylation has been implicated in
208 transcriptional repression [47], we investigated the role of Nse2 and its SUMO ligase activity in
209 Smc5/6 episomal restriction. Depletion of Nse2 had little impact on stability of the other
210 Smc5/6 subunits (Fig. 4a and Extended Data Fig. 6a), confirming that Nse2 is dispensable for
211 the integrity of Smc5/6 [29]. Furthermore, the Nse2-depleted complex was degraded by HBx,
212 indicating that Nse2 is not an essential interaction partner of the viral protein (Extended Data
213 Fig. 6a). However, in the absence of Nse2 the complex showed altered silencing activity (Fig.
214 4a and Extended Data Fig. 6a, lanes 1 and 5). Overexpression of Smc5, to which Nse2 binds,
215 did not rescue the Nse2 depletion phenotype and showed weak dominant-negative effects in
216 wild-type cells, presumably due to titration of Nse2 out of the complex. This indicates that
217 Nse2 is important for restriction. Strikingly, however, the Nse2-depleted complex retained its
218 ability to associate with episomal DNA (Fig. 4b and Extended Data Fig. 6b). This points to

Nse2 acting at a step subsequent to Smc5/6 loading onto DNA. Furthermore, a SUMO ligase-inactive mutant of Nse2 (C215A) [45] was as efficient as the wild-type protein in restoring full restriction activity to the complex in a complementation assay (Fig. 4a and Extended Data Fig. 6a, lanes 5–7). By contrast, the Nse2 mutant was severely compromised in supporting cell growth in a colony formation assay (Fig. 4c). This was unanticipated since the Nse2 SUMO ligase activity is generally viewed as non-essential. However, it is consistent with the slow growth phenotype reported for Nse2-depleted human breast cancer cells [48]. We concluded that Nse2 is important for Smc5/6 restriction while its SUMO ligase activity is not.

Previous studies have shown that Smc5/6 localizes to sub-nuclear structures known as promyelocytic leukemia nuclear bodies (PML-NBs) [49,50]. This co-localization likely has functional implications with respect to Smc5/6 restriction activity. Indeed, depletion of PML and Sp100, two major constituents of PML-NBs, leads to dispersal of Smc5/6 throughout the nucleus and concomitant loss of episomal restriction activity [49]. To examine whether Nse2 has a role in the co-localization of Smc5/6 to PML-NBs, we used confocal fluorescence microscopy. Nse2 formed discrete nuclear foci that co-localized with Sp100 foci in the nucleus of PHH (Fig. 4d, upper panels). Similarly, Smc6 co-localized with PML foci, in line with previous studies (Fig. 4d, middle right panels and Extended Data Fig. 6c) [49,50]. Depletion of Nse2 by siRNA did not affect the co-localization of Smc6 with PML (Fig. 4d, middle panels, compare siCtrl and siNse2), nor did it change the percentage of cells showing Smc6 foci (Fig. 4d, lower panels). Thus, Nse2 is not implicated in Smc5/6 recruitment to PML-NBs. Collectively, these data indicate that restriction by Smc5/6 involves a SUMO ligase-independent function of Nse2 that operates at a step other than episomal DNA binding or localization to PML-NBs.

SLF2 promotes silencing by recruiting Smc5/6 to PML-NBs

In addition to Nse1–Nse4, the yeast Smc5/6 contains two less well-characterized non-SMC subunits named Nse5 and Nse6 [51]. These two proteins form a dimer and associate loosely with the hexameric core Smc5/6 complex through contacts with both Smc5 and Smc6 [52]. The distantly related SLF1 and SLF2 proteins are believed to be the functional human orthologs of yeast Nse5 and Nse6 [53]. Little is known about how the Nse5/6 dimer contributes to Smc5/6 function. In yeast, Nse5/6 appears to play a key role in the recruitment and loading of Smc5/6 onto chromatin, in particular to sites of DSBs and at stalled replication forks [54–56], as well as other chromosomal regions [57]. Similarly, the recruitment of human Smc5/6 to sites of DNA damage has been shown to require the Nse6 ortholog SLF2 and its interaction with SLF1 [53]. To determine whether SLF1 and SLF2 play a role in Smc5/6 restriction, we individually depleted these proteins. Depletion of SLF1 had no effect on the levels of SLF2 and the core Smc5/6 subunits, nor did it alter Smc5/6 binding and silencing of an episomal luciferase reporter (Fig. 5a,b. Depletion of SLF2 also had no effect on Smc5/6 protein stability (Fig. 5a, lanes 1 and 5). However, SLF1 protein levels were reduced, suggesting that SLF1 is stable only in association with SLF2. Strikingly, SLF2-depleted cells showed markedly increased episomal reporter gene activity, indicating loss of silencing (Fig. 5a and Extended Data Fig. 7a, lanes 1 and 5). Moreover, HBx normally degraded Smc5/6 in these cells, arguing against SLF1 or SLF2 being direct interaction partners of HBx, and this had little further effect on transcription of the episomal reporter, consistent with SLF2 acting through the Smc5/6 pathway (Extended Data Fig. 7a). Collectively, these data indicate that SLF2 plays an SLF1-independent role in Smc5/6 restriction activity.

Unexpectedly, ChIP analysis revealed that Smc5/6 still associated with episomal DNA in the absence of SLF2 (Fig. 5b and Extended Data Fig. 7b). Moreover, loss of SLF2 did not impact on cell viability (Fig. 5c). We therefore evaluated whether SLF2 influences Smc5/6 cellular localization. Fluorescence microscopy studies revealed that SLF2 co-localizes with Smc6 in

PML-NBs in PHH (Fig. 5d, upper panels), and that PML-NBs form normally in the absence of SLF2 (Fig. 5d, middle panels). Remarkably, however, depletion of SLF2 led to disappearance of Smc5/6 from PML-NBs (Fig. 5d, middle right panels and Extended Data Fig. 7c). Furthermore, binding of HA-PML to episomal DNA requires the SLF2 subunit of Smc5/6, consistent with the notion that one function of SLF2 is to recruit Smc5/6 and hence episomal DNA to PML-NBs for silencing (Fig. 5e and Extended Data Fig. 7d). Thus, SLF2 is essential for Smc5/6 restriction but, in contrast to its role as a DNA-loading factor [53], SLF2 acts independently of SLF1 to recruit Smc5/6 to PML-NBs.

Discussion

Only Smc5/6 binds to and restricts episomal DNA

In addition to its essential roles in DNA replication and repair, Smc5/6 also functions as a restriction factor against HBV. Smc5/6 binds to and silences the episomal HBV genome and, more generally, any extrachromosomal reporter template [20,21,24]. In this study, we explored the requirements for Smc5/6 to perform its restriction function. A major finding is that binding to and silencing of episomal DNA is unique to Smc5/6 and not a general property of the SMC complexes. This is consistent with previous observations that HBx targets only Smc5/6 for destruction [21]. It is also in agreement with our observations that knockdown of Smc5/6 but not of cohesin or condensin rescues an HBx-deficient HBV in PHH (Extended Data Fig. 1a,b). Thus, Smc5/6 recognizes a feature of episomal DNA templates not detected by the other two SMC complexes.

Role of Smc5/6 ATPase activity in episomal DNA binding

We found that Smc5/6 complexes containing Smc5 or Smc6 subunits defective in ATP binding or hydrolysis all failed to restrict episomal gene expression. However, whereas ATP binding mutants were unable to associate with DNA, consistent with studies in yeast [6], the Smc6 ATP hydrolysis mutant we tested, E1016Q, retained DNA-binding ability. *In vitro* studies suggest that Smc5/6 associates with DNA in a two-step process [6,38,58]. The first step requires ATP binding by Smc5 and Smc6 and involves electrostatic interactions of the complex with the DNA. The second step depends on ATP hydrolysis and leads to the topological entrapment of the DNA within the ring-shaped Smc5/6. A similar mechanism has been proposed for the loading of prokaryotic SMC complexes [59] and of cohesin [60] onto chromosomes. Interestingly, the Smc6 ATP hydrolysis mutant we tested showed reduced binding to episomal DNA templates compared to wild type (Fig. 2d). This suggests that the

hydrolysis mutant complex binds but fails to entrap DNA in its ring structure. However, we cannot exclude that ATP hydrolysis plays a role subsequent to Smc5/6 DNA binding (see below). Nevertheless, these findings provide further evidence that Smc5/6 functions through its binding to the episomal DNA template, and suggest that an ATPase-dependent topological entrapment of the DNA is a prerequisite for silencing.

Role of Nse4 in Smc5/6 binding to episomal DNA

Consistent with previous studies [4,29], we found that Nse4b could physically substitute for Nse4a in the Smc5/6 complex. However, the resulting complex was defective for interaction with episomal DNA templates (Fig. 3). This differs from the situation with the Smc5/6 ATP-hydrolysis mutant, which retained some DNA binding activity, suggesting that Nse4a has essential roles at an early step that precedes entrapment of the DNA and for which Nse4b cannot substitute. Our results may explain previous observations showing that, when overexpressed together with Nse3, Nse4b but not Nse4a stimulated expression of a transiently transfected reporter, and this was dependent on the Nse3-Nse4b interaction [34]. Presumably, overexpressed exogenous Nse4b competes Nse4a out of the complex, thereby preventing binding to and silencing of the episomal reporter. Interestingly, despite being fully defective for episomal silencing, the Nse4b complex was partially competent at supporting normal cell growth. This raises the possibility that Smc5/6 binding to episomal versus chromosomal sites occurs by different mechanisms. It will be interesting to examine if purified Nse4a- and Nse4b-containing Smc5/6 exhibit different DNA substrate preferences *in vitro* [61].

Intriguingly, while Nse4a is expressed in most human tissues [62], expression of Nse4b is restricted to testis [63], and evidence has been presented that in testis Smc5/6 contains Nse4b rather than Nse4a [34]. This raises the question of whether there is any requirement for the testes to express a Smc5/6 devoid of episomal silencing activity.

Nse2 and SLF2 function downstream of Smc5/6 binding

Whereas Smc5, Smc6 and Nse4a all play a key role in Smc5/6 core integrity and binding to episomal DNA, Nse2 and the SLF1/2 (human Nse5/6) sub-complex are dispensable. Nonetheless, Nse2 and SLF2, but not SLF1, are essential for Smc5/6 restriction function. This points to an involvement of Nse2 and SLF2 at a step following Smc5/6 binding to episomal DNA. Indeed, we show that SLF2 is implicated in the co-localization of Smc5/6 to PML-NBs, which are essential for Smc5/6-mediated episomal restriction [49]. Since Smc5/6 binds normally to episomal DNA in the absence of SLF2 (Fig. 5b), we conclude that a major function of SLF2 is to recruit Smc5/6 and, possibly the associated episomal DNA, to PML-NBs. As this occurs independently of SLF1, the process must involve a pathway distinct from that operating at sites of DNA damage, were the recruitment by SLF2 of human Smc5/6 requires its interaction with SLF1 [53]. These findings further implicate PML-NBs in restriction and identify a new role for SLF2 in Smc5/6 activity.

Interestingly, a role for SLF2 and Smc5/6 in mediating repression of unintegrated, circular HIV DNA species has recently been reported [25]. In agreement with our findings, it was shown that SLF1 was not required for SLF2 restriction function. However, in contrast with our data suggesting that SLF2 acts subsequent to Smc5/6 binding to DNA, this study implicates SLF2 in the association of Smc5/6 with the unintegrated viral DNA. We currently have no explanation for the discrepancy. Evidence has been presented that Smc5/6 has similar restriction activity in diverse mammalian cell lines [23]. This makes it unlikely that the inconsistency between the two studies reflects a cell-type specific difference in SLF2 function. Differences in the nature of the episomal templates are also unlikely, as similar unintegrated lentiviral reporter constructs were used in both studies. We note that the two studies measured Smc5/6 binding by ChIP using different HA-tagged subunits (HA-Nse2 by Dupont et al. versus HA-Smc6 in our study). How this might account for the discrepancy

remains unclear. Perhaps the HA tag on Nse2 becomes inaccessible or the protein dissociates from the complex in the absence of SLF2.

Nse2, on the other hand, is required neither for Smc5/6 binding to episomal DNA or for its co-localization to PML-NBs (Fig. 4). This points to a role for Nse2 subsequent to Smc5/6 recruitment to PML-NBs, thus raising the possibility that Nse2 participates directly in transcription silencing in the context of PML-NBs. Surprisingly, we found that Nse2 performs this function independently of its SUMO E3 ligase activity. This was unexpected, given both the fact that the Nse2 E3 ligase plays a role in most of the other Smc5/6 activities [39–41] and the importance of SUMOylation in PML-NB functions [64]. This leads us to conclude that Nse2 contributes to Smc5/6 restriction by performing an unknown function required for silencing that remains to be determined. SMC complexes are dynamic machines able to adopt distinct folded configurations and can undergo conformational changes to perform their functions [65–67]. We speculate that Nse2 may act as an ancillary effector of the Smc5/6 as Nse2 is not essential for the integrity of the complex or for binding to episomal DNA. Nse2 possibly influences Smc5/6 complex interactions with DNA to trigger the silencing function. Notably, Nse2 binds a positively-charged patch on the Smc5 elbow, a region also thought to interact with DNA already loaded into the complex, suggesting interplay between Nse2, Smc5, and the loaded DNA[39]. Furthermore, Nse2 has been reported to possess two SUMO-Interacting Motif (SIM)-like motifs [68]. Nse2 may be recruited to SUMO-conjugated PML through its SIM sequences. Further work is necessary to shed light on these important issues.

Smc5/6 degradation by HBx

Biochemical and structural studies have firmly established that HBx binds to DDB1 to recruit Smc5/6 to the DDB1-containing E3 ligase and induce its degradation [20,22]. However, how

374 HBx interacts with the Smc5/6 complex remains unknown and is of potential therapeutic
375 interest. Single subunit overexpression experiments and yeast two-hybrid interaction assays
376 failed to identify an HBx-interacting partner, suggesting that stable interaction involves more
377 than one Smc5/6 subunit (M.S., unpublished data). We show here that HBx retains its ability
378 to trigger Smc5/6 degradation in the absence of Nse2 or SLF2, or when Nse4b replaces Nse4a
379 in the complex. This argues against these proteins being key ubiquitin substrates or mediating
380 Smc5/6 interaction with HBx. Since SLF2 is responsible for the recruitment of Smc5/6 to
381 PML-NBs, the results also point to HBx triggering degradation of Smc5/6 independently of
382 its co-localization to PML-NBs. HBx efficiently degrades both ATP binding and ATP
383 hydrolysis mutant Smc5/6 complexes. Since Smc5/6 containing Nse4b or defective in ATP
384 binding fail to associate with DNA, we conclude that HBx binds to and triggers degradation
385 of Smc5/6 independently of DNA. Furthermore, Smc5/6, like condensin [67] and cohesin [66], is
386 predicted to adopt distinct conformations during its ATP hydrolysis cycle [4,35,37,58,69]. Our
387 results therefore also point to HBx binding to Smc5/6 regardless of its ATP-dependent
388 conformational state.

389 ***A three-step mechanism of restriction***

390 The exact mechanism whereby Smc5/6 represses episomal gene transcription and the precise
391 nature of the DNA structure recognized by Smc5/6 remain to be determined. It is possible that
392 the binding of Smc5/6 to episomal DNA is topological. Indeed, *in vitro*, the yeast and the
393 human complexes detect and bind DNA tertiary structures displaying crossed DNA helices
394 such as plectonemes and catenated DNA templates using the energy of ATP hydrolysis to
395 promote their compaction[6,61]. Whether the same is true *in vivo* in a cellular context remains to
396 be resolved. The purified human complex used in these studies lacks the Nse2 and SLF2
397 subunits [61], which we found play key roles in restriction. Furthermore, yeast Smc5/6 shows
398 similar compaction and plasmid catenation activities *in vitro* [6,58], yet does not appear to

399 silence episomal DNA templates *in vivo* (M.S., unpublished data). Thus, although ATP
400 hydrolysis is required for restriction (Fig. 2), it is unlikely that Smc5/6 silences episomal gene
401 expression solely by an ATPase-dependent DNA entrapment and/or compaction mechanism.

402 Rather, our findings that Nse2 and SLF2 have distinct roles and act after Smc5/6 binding to
403 episomal DNA would lead us to propose the following three-step silencing mechanism. The
404 first step involves Smc5/6 binding to and, likely, topological entrapment of the episomal
405 DNA template. The second leads to recruitment of Smc5/6 to PML-NBs by SLF2 through a
406 pathway independent of SLF1. The third results in episomal silencing by a mechanism that
407 implicates an Nse2 function other than its SUMO E3 ligase activity. PML-NBs are well
408 known to serve a host antiviral defense function by associating with the genomes of several
409 DNA viruses soon after their delivery into the nucleus to inhibit their expression [70]. It will be
410 interesting to determine whether cells use the same antiviral mechanism to target DNA
411 viruses other than HBV.
412

Acknowledgments

We are most grateful to Thomas Gligoris and Stephan Gruber for help in designing the Smc5 and Smc6 ATPase mutants, to Oscar Fernandez-Capetillo for providing the anti-Nse2 antibody, and to Aurélie Diman, Sari Kassem and Joseph Curran for critical reading of the manuscript. This work was supported by grants from the Swiss National Science Foundation 310030-149626 and 310030-175781 to M.S., by the Canton of Geneva, and by Gilead Sciences.

Author Contributions

F.A., R.K.B., S.P.F. and M.S. conceived the study and designed the experiments. D.R. performed the PHH experiments shown in Extended Data Fig. 1a,b. D.R. and D.K. performed the confocal microscopy experiments shown in Fig. 4d. R.K.B. and D.K. performed the confocal microscopy experiments shown in Fig. 5d. F.A. performed all the other experiments. B.B. contributed to several figures. AD contributed to the revision of the manuscript. All authors interpreted the results. F.A. and M.S. wrote the manuscript with input from all authors.

Competing interests

This study was partly funded by Gilead Sciences, Inc., and D.R., D.K., R.K.B. and S.P.F are employees of Gilead Sciences, Inc. The other authors declare no competing financial interests.

Figure Legends

Fig. 1 | Only Smc5/6, not cohesin or condensin, binds to and silences episomal templates.

a, Schematic diagram illustrating the similar ring-shaped organization of the three SMC complexes, condensin, cohesin and Smc5/6. See text for details. CAP-H is the kleisin counterpart of Nse4 in the Smc2/4 condensin complex [9].

b, HepG2 cells were transduced with lentiviral constructs expressing Cas9 alone (Ctrl) or Cas9 together with single guide RNAs (sgRNA) targeting the indicated Smc subunits. After selection, cells were transfected in parallel with a luciferase reporter plasmid. Luciferase assay and Western blot analysis were performed 5 days later. Luciferase activity is relative to that measured in control cells, which was set to 1. Data are means ± SEM of 5 independent experiments. Statistical significance relative to the control (Ctrl) was calculated by one-way ANOVA with Dunnett's multiple comparison correction; *p=0.014, ***p=0.0008, ns: not significant (p>0.05).

c, Cells depleted as in **b** and complemented with the corresponding HA-epitope tagged Smc subunit were co-transduced with an integrase-defective lentiviral vector to deliver the luciferase reporter as an extrachromosomal DNA [72], and with lentiviruses encoding GFP or GFP-HBx. Binding of the proteins at the indicated regions was monitored 4 days later by ChIP using anti-HA antibodies. Values are expressed as percentage of input DNA recovered. Data are means ± SEM of 2 independent experiments. Statistical significance for each region (actin, cohesin or luciferase) relative to HA-Smc2/GFP transduced cells was calculated with by one-way ANOVA with Dunnett's multiple comparison correction. Only p-values <0.05 are labeled; **p<0.01. Note that in these and subsequent experiments, the complementing HA-Smc6 is typically overexpressed and only the minor fraction assembled into a Smc5/6 complex binds to DNA and is degraded by HBx [20].

Fig. 2 | Smc5 and Smc6 ATP binding and hydrolysis are required for episomal DNA restriction.

a, HepG2 cells depleted of Smc5 (grey bars) or not (black bars) were generated as before. Cells were transfected with a luciferase reporter plasmid, and then transduced with lentiviruses encoding GFP, wild-type Smc5 or the indicated Smc5 ATP binding or ATP hydrolysis mutants. Luciferase assay and western blot analysis were performed 5 days later. Luciferase values are relative to those in non-depleted cells expressing GFP. Data are means ± SEM of 3 independent experiments. Statistical significance relative to matched GFP control was calculated by one-way ANOVA with Dunnett's multiple comparison correction. Only p-values <0.05 are labeled; *p= 0.0211, ***p= 0.0005.

b, Similar experiments as in **a** were performed to test Smc6 derivatives carrying equivalent mutations for functional complementation of Smc6 CRISPR knockout cells. Data are means ± SEM of 5 independent experiments. Statistical significance relative to matched GFP control was calculated by one-way ANOVA with Dunnett's multiple comparison correction. Only p-values <0.05 are labeled; *p= 0.0295, **p= 0.0069.

c, HepG2 cells depleted of Smc6 as in **b** and expressing HA-tagged versions of GFP, wild-type or the indicated ATP-binding mutants of Smc6 were co-transduced with an integrase-defective lentiviral luciferase reporter construct together with lentiviruses encoding GFP or GFP-HBx. Anti-HA ChIP and Western blot analysis were performed 5-6 days later as in Fig. 1b. Data are means ± SEM of 3 independent experiments. Unessential lanes were removed from the original blot images. Statistical significance for luciferase reporter region relative to HA-GFP/GFP control was calculated by one-way ANOVA with Dunnett's multiple comparison correction; †p=0.056, and all other comparisons were p>0.05.

d, Same as **c** but with cells expressing HA-tagged wild type or the indicated Smc6 ATP hydrolysis mutant. Data are expressed as means ± SEM of 3 independent experiments. Statistical significance for luciferase reporter region relative to HA-GFP/GFP control was calculated by one-way ANOVA with Dunnett's multiple comparison correction; Only p-values <0.05 are labeled; *p= 0.0258, **p= 0.0024.

Fig. 3 | Nse4b-containing Smc5/6 complexes support cell viability but fail to silence episomal DNA.

a, HepG2 cells depleted of Nse4a (grey bars) or not (black bars) were transfected with a luciferase reporter plasmid, and shortly after transduced with lentiviruses encoding GFP, Nse4a (long), a shorter splicing isoform of Nse4a (short), or Nse4b as indicated. Luciferase assay and Western blot analysis were performed and are presented as in Fig. 2a. Expression of Nse4b was inferred from its stabilization effect on the other Smc5/6 subunits (lane 8). Data are means ± SEM of 4 independent experiments. Statistical significance relative to matched GFP control was calculated by one-way ANOVA with Dunnett's multiple comparison correction. Only p-values <0.05 are labeled; *p= 0.0120.

b, Control HepG2 cells expressing HA-GFP, or Nse4a-depleted cells expressing HA-Nse4b or HA-Nse4a, were co-transduced with an integrase-defective lentiviral luciferase reporter construct and with lentiviruses encoding GFP or GFP–HBx. Anti-HA ChIP and Western blot analyses were performed 5 days later as before. Data are means ± SEM of 2 independent experiments. Statistical significance for luciferase reporter region relative to HA-GFP/GFP control was calculated by one-way ANOVA with Dunnett's multiple comparison correction. Only p-values <0.05 are labeled; *p= 0.0455, ****p<0.0001.

c, Colony formation assay. Control HepG2 cells and cells depleted of Nse4a were either mock-transduced or transduced with lentiviral constructs expressing the indicated proteins. Cells were then seeded at low density and grown under selective conditions for 14-21 days prior to fixation and staining with crystal violet. Shown is one representative experiment out of three performed.

Fig. 4 | Nse2 but not its SUMO ligase is essential for episomal restriction but not for Smc5/6 DNA binding and co-localization with PML bodies.

a, Control HepG2 cells (black bars) and cells depleted of Nse2 (grey bars) were transfected with a luciferase reporter plasmid, and subsequently transduced with lentiviruses encoding GFP, Flag-tagged wild-type Nse2 (F-Nse2) or a Nse2-SUMO E3 ligase-defective mutant (C215A) [45], or Smc5. Luciferase assay and Western blot analysis were performed as before. Luciferase values are relative to GFP in control cells. Data are means ± SEM of 4 independent experiments. Statistical significance relative to matched GFP control was calculated by one-way ANOVA with Dunnett's multiple comparison correction. Only p-values <0.05 are labeled; **p<0.01, ***p= 0.0005.

b, HepG2 cells depleted of Smc6 and expressing HA-tagged Smc6 were transduced with lentiviral constructs expressing Cas9 alone (ctrl) or Cas9 together with a sgRNA targeting Nse2. Cells were then co-transduced with an integrase-defective lentiviral luciferase reporter construct and with lentiviruses encoding GFP, GFP-HBx or Flag-tagged Nse2. Anti-HA ChIP and Western blot analysis were performed 5 days later as before. Data are means ± SEM of 3 independent experiments. Statistical significance for luciferase reporter region relative to GFP control (Ctrl) was calculated by one-way ANOVA with Dunnett's multiple comparison correction. Only p-values <0.05 are labeled; ****p<0.0001.

c, Colony formation assay of control HepG2 cells or cells depleted of Nse2 and expressing the indicated proteins from lentiviral vectors. Shown is one representative experiment out of three performed.

d, Confocal images of PHH transfected with either a non-targeting control siRNA (siCtrl) or with siRNA against Nse2 (siNse2) and incubated for 13 days. Cells were stained for Sp100 or Smc6 (green) and for Nse2 or PML (red) as indicated. The boundaries of nuclei are outlined in white circles based on DAPI signal (not shown). The bottom graphs reflect the percentage of nuclei without (left) or with (right) Smc6 foci. The data represent the mean ± SD of 2 independent experiments, with 328-428 nuclei analyzed per siRNA treatment in each experiment. Statistical significance relative to siCtrl was calculated by paired t-test; ns: not significant ($p>0.05$).

Fig. 5 | SLF2 promotes silencing by recruiting Smc5/6 to PML-NBs

a, HepG2 cells were transduced with lentiviral constructs expressing Cas9 alone (ctrl), or Cas9 together with sgRNA as indicated. Cells were transfected with a luciferase reporter plasmid and transduced with GFP or GFP-HBx. Analyses were performed as before. Data are means ± SEM of 3 independent experiments. Statistical significance relative to Ctrl was calculated by one-way ANOVA with Dunnett's multiple comparison correction. Only p-values <0.05 are labeled; ***$p<0.001$.

b, Smc6-depleted HepG2 cells expressing HA-tagged Smc6 were transduced with constructs expressing Cas9 alone (Ctrl), or Cas9 together with sgRNA as indicated. Cells were co-transduced with an integrase-defective luciferase lentivirus and with the indicated lentiviruses. Analyses were as before. Data are mean ± SEM of 2 independent experiments.

Statistical significance for luciferase region relative to Ctrl-GFP was calculated by one-way ANOVA with Dunnett's multiple comparison correction. Only p-values <0.05 are labeled; **p= 0.0042.

c, Colony formation assay of control HepG2 cells or cells depleted of SLF2 and transduced with lentiviruses encoding either GFP or SLF2.

d, Confocal images of PHH transfected with either a control siRNA (siCtrl) or with siRNA against SLF2 (siSLF2) and incubated for 13 days. Cells were stained for Sp100 or Smc6 (green) and for SLF2 or PML (red) as indicated. Data are presented as in Fig. 4d and are mean ± SD of 3 independent experiments, with 56-119 nuclei analyzed per siRNA treatment in each experiment. Statistical significance relative to siCtrl was calculated by paired t-test; *p= 0.0156, **p= 0.0027.

e, HepG2 cells expressing HA-PML-1 were transduced with lentiviral constructs expressing Cas9 alone (Ctrl), or Cas9 together with sgRNA targeting SLF2. Cells were co-transduced with an integrase-defective luciferase lentivirus and with lentiviruses expressing GFP, ICP0 (a protein from herpes simplex virus type 1 known to induces PML degradation [73]), SLF2 or HBx. Analyses were as before. Data are mean ± SEM of 4 independent experiments with n=4 for all conditions except for HBx n=3. Statistical significance for luciferase region relative to Ctrl-GFP was calculated by one-way ANOVA with Dunnett's multiple comparison correction. Only p-values <0.05 are labeled; *p<0.05, **p<0.01, ***p<0.001.

References

1. Jeppsson, K., Kanno, T., Shirahige, K. & Sjögren, C. The maintenance of chromosome structure: positioning and functioning of SMC complexes. *Nat. Rev. Mol. Cell Biol.* **15**, 601–614 (2014).
2. Gligoris, T. & Löwe, J. Structural Insights into Ring Formation of Cohesin and Related Smc Complexes. *Trends Cell Biol.* **26**, 680–693 (2016).
3. Alt, A. *et al.* Specialized interfaces of Smc5/6 control hinge stability and DNA association. *Nat. Commun.* **8**, 14011 (2017).
4. Adamus, M. *et al.* Molecular Insights into the Architecture of the Human SMC5/6 Complex. *J. Mol. Biol.* **432**, 3820–3837 (2020).
5. Palecek, J., Vidot, S., Feng, M., Doherty, A. J. & Lehmann, A. R. The Smc5-Smc6 DNA repair complex: Bridging of the Smc5-Smc6 heads by the kleisin, nse4, and non-kleisin subunits. *J. Biol. Chem.* **281**, 36952–36959 (2006).
6. Kanno, T., Berta, D. G. & Sjögren, C. The Smc5/6 Complex Is an ATP-Dependent Intermolecular DNA Linker. *Cell Rep.* **12**, 1471–1482 (2015).
7. Aragón, L. The Smc5/6 Complex: New and Old Functions of the Enigmatic Long-Distance Relative. *Annu. Rev. Genet.* **52**, 89–107 (2018).
8. Palecek, J. J. SMC5/6: Multifunctional Player in Replication. *Genes* **10**, 7 (2019).
9. Palecek, J. J. & Gruber, S. Kite Proteins: a Superfamily of SMC/Kleisin Partners Conserved Across Bacteria, Archaea, and Eukaryotes. *Structure* **23**, 2183–2190 (2015).
10. De Piccoli, G. *et al.* Smc5-Smc6 mediate DNA double-strand-break repair by promoting sister-chromatid recombination. *Nat. Cell Biol.* **8**, 1032–1034 (2006).
11. Potts, P. R., Porteus, M. H. & Yu, H. Human SMC5/6 complex promotes sister chromatid homologous recombination by recruiting the SMC1/3 cohesin complex to double-strand breaks. *EMBO J.* **25**, 3377–3388 (2006).
12. Ampatzidou, E., Irmisch, A., O'Connell, M. J. & Murray, J. M. Smc5/6 Is Required for Repair at Collapsed Replication Forks. *Mol. Cell. Biol.* **26**, 9387–9401 (2006).
13. Betts Lindroos, H. *et al.* Chromosomal Association of the Smc5/6 Complex Reveals that It Functions in Differently Regulated Pathways. *Mol. Cell* **22**, 755–767 (2006).

14. Menolfi, D., Delamarre, A., Lengronne, A., Pasero, P. & Branzei, D. Essential Roles of the Smc5/6 Complex in Replication through Natural Pausing Sites and Endogenous DNA Damage Tolerance. *Mol. Cell* **60**, 835–846 (2015).
15. Li, X. & Heyer, W.-D. Homologous recombination in DNA repair and DNA damage tolerance. *Cell Res.* **18**, 99–113 (2008).
16. Bermúdez-López, M. *et al.* The Smc5/6 complex is required for dissolution of DNA-mediated sister chromatid linkages. *Nucleic Acids Res.* **38**, 6502–6512 (2010).
17. Kegel, A. & Sjögren, C. The Smc5/6 complex: More than repair? *Cold Spring Harb. Symp. Quant. Biol.* **75**, 179–187 (2010).
18. Jeppsson, K. *et al.* The Chromosomal Association of the Smc5/6 Complex Depends on Cohesion and Predicts the Level of Sister Chromatid Entanglement. *PLOS Genet* **10**, e1004680 (2014).
19. Kegel, A. *et al.* Chromosome length influences replication-induced topological stress. *Nature* **471**, 392–396 (2011).
20. Decorsière, A. *et al.* Hepatitis B virus X protein identifies the Smc5/6 complex as a host restriction factor. *Nature* **531**, 386–389 (2016).
21. Murphy, C. M. *et al.* Hepatitis B Virus X protein promotes degradation of SMC5/6 to enhance HBV replication. *Cell Rep.* **16**, 2846–2854 (2016).
22. Li, T., Robert, E. I., van Breugel, P. C., Strubin, M. & Zheng, N. A promiscuous α-helical motif anchors viral hijackers and substrate receptors to the CUL4–DDB1 ubiquitin ligase machinery. *Nat. Struct. Mol. Biol.* **17**, 105–112 (2010).
23. Abdul, F. *et al.* Smc5/6 Antagonism by HBx Is an Evolutionarily Conserved Function of Hepatitis B Virus Infection in Mammals. *J. Virol.* **92**, e00769-18 (2018).
24. van Breugel, P. C. *et al.* Hepatitis B virus X protein stimulates gene expression selectively from extrachromosomal DNA templates. *Hepatology* **56**, 2116–2124 (2012).
25. Dupont, L. *et al.* The SMC5/6 complex compacts and silences unintegrated HIV-1 DNA and is antagonized by Vpr. *Cell Host Microbe* **29**, 792-805.e6 (2021).
26. Gibson, R. T. & Androphy, E. J. The SMC5/6 Complex Represses the Replicative Program of High-Risk Human Papillomavirus Type 31. *Pathogens* **9**, 786 (2020).
27. Nagy, G. *et al.* Motif oriented high-resolution analysis of ChIP-seq data reveals the topological order of CTCF and cohesin proteins on DNA. *BMC Genomics* **17**, 637 (2016).

628 28. Sutani, T. *et al.* Condensin targets and reduces unwound DNA structures associated with transcription in
629 mitotic chromosome condensation. *Nat. Commun.* **6**, 7815 (2015).
630 29. Taylor, E. M., Copsey, A. C., Hudson, J. J. R., Vidot, S. & Lehmann, A. R. Identification of the proteins,
631 including MAGEG1, that make up the human SMC5-6 protein complex. *Mol. Cell. Biol.* **28**, 1197–1206
632 (2008).
633 30. Harvey, S. H., Krien, M. J. & O'Connell, M. J. Structural maintenance of chromosomes (SMC) proteins, a
634 family of conserved ATPases. *Genome Biol.* **3**, reviews3003.1 (2002).
635 31. Arumugam, P. *et al.* ATP Hydrolysis Is Required for Cohesin's Association with Chromosomes. *Curr. Biol.*
636 **13**, 1941–1953 (2003).
637 32. Hirano, M., Anderson, D. E., Erickson, H. P. & Hirano, T. Bimodal activation of SMC ATPase by intra-
638 and inter-molecular interactions. *EMBO J.* **20**, 3238–3250 (2001).
639 33. Guerineau, M. *et al.* Analysis of the Nse3/MAGE-binding domain of the Nse4/EID family proteins. *PloS*
640 *One* **7**, e35813 (2012).
641 34. Hudson, J. J. R. *et al.* Interactions between the Nse3 and Nse4 Components of the SMC5-6 Complex
642 Identify Evolutionarily Conserved Interactions between MAGE and EID Families. *PLOS ONE* **6**, e17270
643 (2011).
644 35. Vondrova, L. *et al.* A role of the Nse4 kleisin and Nse1/Nse3 KITE subunits in the ATPase cycle of
645 SMC5/6. *Sci. Rep.* **10**, 9694 (2020).
646 36. Venegas, A. B., Natsume, T., Kanemaki, M. & Hickson, I. D. Inducible Degradation of the Human SMC5/6
647 Complex Reveals an Essential Role Only during Interphase. *Cell Rep.* **31**, 107533 (2020).
648 37. Jo, A., Li, S., Shin, J. W., Zhao, X. & Cho, Y. Structure Basis for Shaping the Nse4 Protein by the Nse1 and
649 Nse3 Dimer within the Smc5/6 Complex. *J. Mol. Biol.* **433**, 166910 (2021).
650 38. Zabrady, K. *et al.* Chromatin association of the SMC5/6 complex is dependent on binding of its NSE3
651 subunit to DNA. *Nucleic Acids Res.* **44**, 1064–1079 (2016).
652 39. Duan, X. *et al.* Structural and Functional Insights into the Roles of the Mms21 Subunit of the Smc5/6
653 Complex. *Mol. Cell* **35**, 657–668 (2009).
654 40. Solé-Soler, R. & Torres-Rosell, J. Smc5/6, an atypical SMC complex with two RING-type subunits.
655 *Biochem. Soc. Trans.* **48**, 2159–2171 (2020).
656 41. Zhao, X. & Blobel, G. A SUMO ligase is part of a nuclear multiprotein complex that affects DNA repair
657 and chromosomal organization. *Proc. Natl. Acad. Sci. U. S. A.* **102**, 4777–4782 (2005).

42. Jacome, A. *et al.* NSMCE2 suppresses cancer and aging in mice independently of its SUMO ligase activity. *EMBO J.* **34**, 2604–2619 (2015).
43. Andrews, E. A. *et al.* Nse2, a Component of the Smc5-6 Complex, Is a SUMO Ligase Required for the Response to DNA Damage. *Mol. Cell. Biol.* **25**, 185–196 (2005).
44. Pond, K. W., de Renty, C., Yagle, M. K. & Ellis, N. A. Rescue of collapsed replication forks is dependent on NSMCE2 to prevent mitotic DNA damage. *PLoS Genet.* **15**, (2019).
45. Potts, P. R. & Yu, H. Human MMS21/NSE2 is a SUMO ligase required for DNA repair. *Mol. Cell. Biol.* **25**, 7021–7032 (2005).
46. Zapatka, M. *et al.* Sumoylation of Smc5 Promotes Error-free Bypass at Damaged Replication Forks. *Cell Rep.* **29**, 3160-3172.e4 (2019).
47. Boulanger, M., Chakraborty, M., Tempé, D., Piechaczyk, M. & Bossis, G. SUMO and Transcriptional Regulation: The Lessons of Large-Scale Proteomic, Modifomic and Genomic Studies. *Mol. Basel Switz.* **26**, 828 (2021).
48. Ni, H. J. *et al.* Depletion of SUMO ligase hMMS21 impairs G1 to S transition in MCF-7 breast cancer cells. *Biochim. Biophys. Acta - Gen. Subj.* **1820**, 1893–1900 (2012).
49. Niu, C. *et al.* The Smc5/6 Complex Restricts HBV when Localized to ND10 without Inducing an Innate Immune Response and Is Counteracted by the HBV X Protein Shortly after Infection. *PLOS ONE* **12**, e0169648 (2017).
50. Potts, P. R. & Yu, H. The SMC5/6 complex maintains telomere length in ALT cancer cells through SUMOylation of telomere-binding proteins. *Nat. Struct. Mol. Biol.* **14**, 581–590 (2007).
51. Pebernard, S., Wohlschlegel, J., McDonald, W. H., Yates, J. R., 3rd & Boddy, M. N. The Nse5-Nse6 dimer mediates DNA repair roles of the Smc5-Smc6 complex. *Mol. Cell. Biol.* **26**, 1617–1630 (2006).
52. Yu, Y. *et al.* Integrative analysis reveals unique structural and functional features of the Smc5/6 complex. *Proc. Natl. Acad. Sci.* **118**, (2021).
53. Räschle, M. *et al.* Proteomics reveals dynamic assembly of repair complexes during bypass of DNA cross-links. *Science* **348**, 1253671 (2015).
54. Bustard, D. E. *et al.* During replication stress, non-Smc element 5 (Nse5) is required for Smc5/6 protein complex functionality at stalled forks. *J. Biol. Chem.* **287**, 11374–11383 (2012).
55. Leung, G. P., Lee, L., Schmidt, T. I., Shirahige, K. & Kobor, M. S. Rtt107 is required for recruitment of the SMC5/6 complex to DNA double strand breaks. *J. Biol. Chem.* **286**, 26250–26257 (2011).

56. Oravcová, M. *et al.* Brc1 Promotes the Focal Accumulation and SUMO Ligase Activity of Smc5-Smc6 during Replication Stress. *Mol. Cell. Biol.* **39**, (2019).
57. Etheridge, T. J. *et al.* Live-cell single-molecule tracking highlights requirements for stable Smc5/6 chromatin association in vivo. *eLife* **10**, e68579 (2021).
58. Gutierrez-Escribano, P. *et al.* Purified Smc5/6 Complex Exhibits DNA Substrate Recognition and Compaction. *Mol. Cell* **80**, 1039-1054.e6 (2020).
59. Wilhelm, L. *et al.* SMC condensin entraps chromosomal DNA by an ATP hydrolysis dependent loading mechanism in Bacillus subtilis. *eLife* **4**, e06659 (2015).
60. Hu, B. *et al.* ATP hydrolysis is required for relocating cohesin from sites occupied by its Scc2/4 loading complex. *Curr. Biol.* **21**, 12–24 (2011).
61. Serrano, D. *et al.* The Smc5/6 Core Complex Is a Structure-Specific DNA Binding and Compacting Machine. *Mol. Cell* **80**, 1025-1038.e5 (2020).
62. Hu, B. *et al.* Qri2/Nse4, a component of the essential Smc5/6 DNA repair complex. *Mol. Microbiol.* **55**, 1735–1750 (2005).
63. Båvner, A., Matthews, J., Sanyal, S., Gustafsson, J.-Å. & Treuter, E. EID3 is a novel EID family member and an inhibitor of CBP-dependent co-activation. *Nucleic Acids Res.* **33**, 3561–3569 (2005).
64. Corpet, A. *et al.* PML nuclear bodies and chromatin dynamics: catch me if you can! *Nucleic Acids Res.* **48**, 11890–11912 (2020).
65. Bauer, B. W. *et al.* Cohesin mediates DNA loop extrusion by a "swing and clamp" mechanism. *Cell* **184**, 5448-5464.e22 (2021).
66. Bürmann, F. *et al.* A folded conformation of MukBEF and cohesin. *Nat. Struct. Mol. Biol.* **26**, 227–236 (2019).
67. Lee, B. G. *et al.* Cryo-EM structures of holo condensin reveal a subunit flip-flop mechanism. *Nat. Struct. Mol. Biol.* **27**, 743–751 (2020).
68. Varejão, N. *et al.* Structural basis for the E3 ligase activity enhancement of yeast Nse2 by SUMO-interacting motifs. *Nat. Commun.* **12**, 7013 (2021).
69. Bermúdez-López, M. *et al.* ATPase-Dependent Control of the Mms21 SUMO Ligase during DNA Repair. *PLOS Biol.* **13**, e1002089 (2015).
70. Everett, R. D. The Spatial Organization of DNA Virus Genomes in the Nucleus. *PLOS Pathog.* **9**, e1003386 (2013).

71. Sanjana, N. E., Shalem, O. & Zhang, F. Improved vectors and genome-wide libraries for CRISPR screening. *Nat. Methods* **11**, 783–784 (2014).

72. Michelini, Z., Negri, D. & Cara, A. Integrase defective, nonintegrating lentiviral vectors. *Methods Mol. Biol. Clifton NJ* **614**, 101–110 (2010).

73. Cuchet-Lourenço, D., Vanni, E., Glass, M., Orr, A. & Everett, R. D. Herpes simplex virus 1 ubiquitin ligase ICP0 interacts with PML isoform I and induces its SUMO-independent degradation. *J. Virol.* **86**, 11209–11222 (2012).

Methods

Cell Lines and Culture Conditions

The cell lines used in this study were the human embryonic kidney (HEK) cell line HEK 293T/17 (ATCC CRL-11268), the human hepatoma cell line HepG2 (ATCC HB-8065) and HeLa. All cell lines and their derivatives were grown at 37°C under 5% CO2 in Dulbecco modified Eagle medium (DMEM) (Gibco) supplemented with 10% (v/v) fetal calf serum (Gibco), 1% (v/v) penicillin/streptomycin solution, 2 mM l-glutamine, 1 mM sodium pyruvate, and 0.1 mM MEM non-essential amino acids solution (all from Life Technologies).

Primary Human Hepatocytes

Primary human hepatocytes (PHH) isolated from deceased donor livers were purchased from BioIVT (Westbury, NY) and maintained in William's E medium with added supplements as specified by the vendor. Consent was obtained from the donor or the donor's legal next of kin for use of the samples and their derivatives for research purposes using institutional review board (IRB)-approved authorizations.

Expression Plasmids, Complementing Constructs and Smc5/6 Subunit Mutants

GFP and GFP-HBx were expressed from the lentiviral vector pWPT (Addgene #12255) as described [20]. All wild-type and mutant Smc5/6 complex subunits and naturally occurring isoforms thereof were produced by cloning human codon-optimized, chemically synthesized (System Biosciences) gene sequences into pCDH-CMV-MCS-EF1α-copGFP lentiviral vector (System Biosciences #CD511B) under control of the CMV promoter. Complementing constructs resistant to CRISPR/Cas9 cleavage were generated by inserting silent mutations in the region of the mRNA covered by the sgRNA. The Smc5(K86E) and Smc6(K82E) point mutations in the Walker A nucleotide-binding motif, and the Smc5(D1019A) and Smc6(D1015A) mutations in the Walker B motif, are predicted to abolish ATP binding [31].

The Smc5(E1020A), Smc6(E1016A) and Smc6(E1016Q) substitutions in the Walker B motif are predicted to prevent hydrolysis of the bound ATP [30–32]. DNA sequences of the mutants are available upon request. The secreted Gaussia luciferase (GLuc) used as reporter was expressed from pCMV-GLuc (New England BioLabs) for transient transfection and from pCDH-CMV-Gluc-EF1α-copGFP when delivered as episomal DNA using an integrase-defective (D116A) lentiviral vector.

Gene knockout was performed using the puromycin-resistant CRISPR-Cas9 lentiviral vector plentiCRISPR v2 (Addgene plasmid #52961) encoding Cas9 and containing two BsmBI cloning sites for insertion of single-guide RNA (sgRNA) [71]. The sgRNA sequences specific to the genes of interest were selected using the online CRISPR-Cas9 Design Tool hosted by the Feng Zhang Laboratory (http://crispr.mit.edu), Chopchop (http://chopchop.cbu.uib.no/) or CRISPOR (http://crispor.tefor.net/), and cloned as annealed oligonucleotides into plentiCRISPR v2 as described [71]. The sgRNA sequences used in this study are listed in Supplementary Table 1.

Lentivirus Production and Titration

VSV-G pseudotyped recombinant lentiviruses were produced by transient transfection of HEK 293T/17 cells using the calcium phosphate method. Briefly, $4.5x10^6$ cells were plated in a 10-cm dish and transfected 16 h later with 15 µg lentiviral vector plasmid, 10 µg of packaging plasmid psPAX2 (Addgene plasmid #12260), and 5 µg of envelope plasmid pMD2G (Addgene plasmid #12259). For production of integrase-defective lentiviruses, psPAX2 was replaced by p8.9NdSB (gift from Jeremy Luban) encoding a catalytically inactive integrase point mutant (D116A). The culture medium was changed 8 h post-transfection. Viral containing supernatants were collected 48 h later, filtered through PVDF 0.45 µm filters (Merck-Millipore) and stored at -80°C. The titer of lentiviruses expressing

GFP was estimated by infection of HeLa cells with serially diluted viral supernatants and FACS analysis 4 days later for GFP-positive cells.

Transfection, Transduction, CRISPR-Cas9 Knockout and Complementation Assay

HepG2 cells were typically seeded at a density of 3-6 × 10^5 cells per well of a 6-well dish and transduced the next day with sgRNA-expressing lentiviruses or with the empty parental plentiCRISPR v2 as indicated in the figures. After five days of culture, transduced cells were selected with 5 µg/mL puromycin (Invivogen) for 24 h. Cells were then trypsinized, counted, replated in 6-well dishes at a density of 3-6 × 10^5 cells per well, and immediately reverse-transfected with 15-30 ng of the luciferase reporter plasmid pCMV-GLuc and 1-2 µg of empty EBS-PL vector [20]. Transfection was performed using X-tremeGENE HP DNA transfection reagent (Roche) or polyethylenimine (PEI; Polysciences #23966) following the manufacturer's instructions. Where indicated, cells were then transduced 2 h later with control or complementing lentiviral constructs, and/or with GFP or GFP-HBx. For ChIP and pull down experiments, cells were first transduced with HA-tagged versions of the proteins of interest and 5 days later with sgRNAs targeting the corresponding endogenous protein. Experiments with HA-tagged Smc6 were either performed as described above (Fig. 1c and Extended Data Figs. 1c,d and 2), or starting with a CRISPR/Cas9-edited HepG2 cell clone (6.1.2) isolated following standard methods and expressing low levels of endogenous Smc6 leading to loss of restriction activity but normal cell growth. After expansion under puromycin selection, 2-5 × 10^6 cells were seeded onto one 10- to 15-cm culture dish and transduced the following day with luciferase reporter gene GLuc delivered as an episomal DNA using an integrase-defective (D116A) lentivirus, and with GFP or GFP-HBx as indicated.

Luciferase Reporter Gene Assay

Luciferase activities were measured 4-6 days after reporter transfection or transduction. Five µL of culture supernatants were mixed with 50 µL of GLuc assay buffer (100 mM NaCl, 35 mM EDTA, 0.1% Tween 20, 300 mM sodium ascorbate, 4 µM coelenterazine in 1X phosphate-buffered saline [PBS]) and luminescence was immediately measured in triplicates in a 96 microplate luminometer (Glomax; Promega).

Western Blotting

Cells were lysed in 2% SDS in water, and the lysates were briefly sonicated and denatured at 95°C for 5 minutes. Protein concentrations were estimated using the Pierce™ BCA Protein Assay kit (Thermo Scientific). Proteins (20 µg) were separated on 8-18% SDS-PAGE gradient gels and electroblotted onto nitrocellulose membranes. The membranes were blocked in 5% (w/v) milk – TBST 0.1% [TBS buffer (10 mM Tris-HCl (pH 7.5), 500 mM NaCl) supplemented with 0.1% Tween-20] and probed with primary antibodies overnight at 4˚C in 5% milk – TBST 0.1%. The membranes were then washed thrice with TBST 0.1% for 10 min, and incubated with secondary antibodies for 1 h at RT. The membranes were finally washed thrice with TBST 0.1% for 10 min. Detection was performed with SuperSignal West Pico PLUS chemiluminiscent substrate (Thermo Scientific, 34580) according to the manufacturer's protocol. Images were acquired with the ChemicDoc XRS luminescence imager from Bio-Rad. The primary and secondary antibodies used are listed in Supplementary Table 2.

ChIP and Quantitative PCR

For ChIP experiments, the episomal DNA template was delivered using an integrase-defective lentiviral construct to increase the fraction of cells containing an episomal template and limit the copy number per cell. ChIP analysis was performed using chromatin extracted from about 4-10 × 10^6 HA-tagged protein-expressing HepG2 cells cultured in a 10-15 cm diameter dish.

Cells were harvested with trypsin-EDTA and collected by low-speed centrifugation. Cells were rinsed twice with ice-cold PBS, resuspended and fixed for 45 min with the protein–protein crosslinker ChIP Cross-link Gold (Diagenode) following the manufacturer's instructions, rinsed again twice with ice-cold PBS, and further fixed with 1% formaldehyde (Sigma Aldrich) for 10 min at RT before quenching with 330 mM glycine. After two further washes with ice-cold PBS, cells were resuspended and lysed for 10 min at 4°C in 1 mL Nuclear Extraction buffer (10 mM Tris-HCl (pH 8.0), 10 mM NaCl, 0.5% NP-40) supplemented with EDTA-free protease inhibitor cocktail (Roche). The nuclei were recovered by centrifugation at 500 *g* for 5 min at 4°C and washed once in the same buffer. Nuclei were resuspended in 100 µL FA-lysis buffer (50 mM HEPES/KOH (pH 7.5), 140 mM NaCl, 1 mM EDTA, 1% Triton X-100, 0.1% sodium deoxycholate, protease inhibitor cocktail) containing 1% SDS and incubated for 10 min at RT. After addition of another 100 µL FA-lysis buffer, the mixture was transferred to 1.5 ml bioruptor microtubes (Diagenode) and sonicated using a Bioruptor Pico water bath sonicator (Diagenode) for 10 cycles (30 s ON and 30 s OFF, 4°C). The sonicated lysates were clarified by centrifugation at 16,000 *g* for 10 min. The supernatants were collected and 20 µL (1/10) was set aside as input controls. The rest was mixed in 800 µl FA-lysis buffer supplemented with protease inhibitors with 40 µL packed bead volume of protein A-Sepharose CL-4B (GE Healthcare) coupled to 4 µL anti-HA antibodies (HA.11, clone 16B12, ENZ-ABS118, Enzo Life Sciences) and pre-incubated in FA-lysis buffer with sonicated salmon sperm DNA and BSA. After an overnight incubation at 4°C under constant rotation, the beads were sedimented by brief centrifugation. The beads were washed twice with 1 mL FA-lysis buffer, twice with high-salt buffer (50 mM HEPES-KOH (pH 7.5), 500 mM NaCl, 1 mM EDTA, 1% Triton X-100, 0.1% sodium deoxycholate), twice with LiCl buffer (10 mM Tris-HCl (pH 8.0), 1 mM EDTA, 250 mM LiCl, 1% NP-40, and 1% sodium deoxycholate) and once with TE buffer (10 mM Tris-HCl (pH 8.0), 1 mM

EDTA). Bound protein–DNA complexes were eluted from beads by incubation for 10 min at 65°C in 200 µL elution buffer (50 mM Tris-HCl (pH 8.0), 1% SDS, 10 mM EDTA). After addition of 200 µL TE buffer and 60 µg proteinase K (Eurobio Scientific), DNA crosslinks were reversed by overnight incubation at 65°C. Samples were extracted twice with phenol–chloroform, once with chloroform, and then ethanol precipitated and resuspended in TE buffer. The input DNA treated identically and the recovered DNA were quantified by real-time PCR using the KAPA SYBR FAST qPCR Kit Master Mix (2X) Universal (Kapa Biosystems) and the Bio-Rad CFX96 Real-time PCR System. The values shown in the figures are the ratios between the ChIP signals and the respective input DNA signals. All data are representative of at least two independent experiments. The oligonucleotide primers used are listed in Supplementary Table 3.

Co-Immunoprecipitation

Whole cell extracts were prepared from the same HepG2 cells expressing HA-tagged proteins in a CRISPR/Cas9 knockout background as used in the ChIP experiments shown in Figs 1c and 2c. About 3-4 × 10^6 cells were collected from a 10 cm diameter dish using trypsin-EDTA and pelleted by low-speed centrifugation. Cell were washed once with ice-cold PBS and resuspended in 400 µL of co-immunoprecipitation (co-IP) lysis buffer (50 mM HEPES-KOH (pH 7.5), 150 mM NaCl, 5 mM KCl, 5 mM $MgCl_2$, 50 µM $ZnCl_2$, 0.1% IGEPAL (Sigma-Aldrich CA-630)) supplemented with protease inhibitor cocktail (Roche). The lysates were clarified by centrifugation at 16 000 g for 20 min at 4°C. The supernatants were collected and 40 µl (1/10) was set aside as input controls. The rest was mixed in 600 µl of co-IP lysis buffer with 40 µL packed-bead volume of protein A-Sepharose CL-4B (GE Healthcare) coupled to 3 µL of anti-HA antibody (HA.11, clone 16B12, ENZ-ABS118, Enzo Life Sciences). After 4 h of incubation at 4°C under constant rotation, the beads were sedimented by brief centrifugation (1 min at 300 g) and the supernatant was discarded. The beads were washed 3

872 times with 1 mL of co-IP lysis buffer. Bound protein-protein complexes were released from
873 the beads by addition of 20 µL of 2× Laemmli SDS sample buffer. The inputs and eluted
874 proteins were analysed by immunoblotting.

875 ***Colony Formation Assay***

876 HepG2 cells were transduced with puromycin-resistant plentiCRISPR v2 lentiviruses
877 expressing gene-specific sgRNAs or no sgRNA (Ctrl) as indicated in the figures. Four days
878 after transduction, cells were selected with 5 µg/mL puromycin (Invivogen). One day later,
879 cells were seeded at low density in twelve-well plates, transduced with lentiviral constructs
880 encoding the indicated proteins, and further cultured for 14-21 days under puromycin
881 selection. Resistant colonies were fixed and stained with 0.05% crystal violet.

882 ***RNA interference and HBV infection of PHH***

883 PHH were transfected with 10-50 nM siRNA using Lipofectamine RNAiMax according to the
884 manufacturer's instructions (Life Technologies). The PHH media was refreshed 24 hours post-
885 transfection. For confocal microscopy, PHH were further incubated for 13 days before fixing
886 and staining. In Extended Data Fig. 1a, PHH were incubated for 3 days post-transfection
887 before infecting with wild-type (WT) or HBx-deficient (ΔX) HBV (1,000 genomic
888 equivalents/cell) as described [49]. Production of HBV(WT) and HBV(ΔX) virions (genotype
889 D) from, respectively, HepAD38 and HepG2-H1.3x- stable cell lines was performed as
890 previously described [20,49].

891 ***Immunostaining and Confocal Microscopy***

892 PHH were seeded onto glass coverslips (Corning BioCoat Poly-D-Lysine/Laminin 12 mm,
893 Corning, NY) in 12-well Corning CellBind plates. At the end of treatment, cells were fixed
894 with Perfusion Fixative Reagent (ThermoFisher Scientific) for 10 min and washed three times
895 in Dulbecco's Phosphate-Buffered Salt Solution (DPBS) (Corning). Immunostaining was

performed at RT. Cells were permeabilized in 0.3% Triton X-100 (MilliporeSigma) for 15 min following by blocking in DPBS with 3% bovine serum albumin (BSA) (MilliporeSigma) and 10% HyClone Fetal Bovine Serum (FBS) (MilliporeSigma) for 60 min. The final concentrations of primary antibodies were 0.2 μg/ml rabbit anti-Nse2 polyclonal antibody (ThermoFisher Scientific, PA5-65676), 1 μg/ml mouse monoclonal anti-Smc6 antibody (AT3956a), 4.44 μg/ml rabbit anti-PML antibody (Novus Biologicals, NB100-59787), 10 μg/ml mouse polyclonal anti-Sp100 antibody (Abcam, ab167605), and 1 μg/ml rabbit polyclonal anti-SLF2 antibody (Abcam, ab122480). Secondary antibodies conjugated with either Alexa Fluor 488 donkey anti-mouse IgG, ThermoFisher Scientific, A21202), or Alexa Fluor 647 goat anti-rabbit IgG (H+L), ThermoFisher Scientific, A32733) were used at 2 μg/ml. All antibodies were diluted in DPBS supplemented with 1.5% BSA. Primary and secondary antibodies were applied for 90 min and 60 min, respectively. The coverslips with stained cells were mounted on glass microscopic slides (VWR International, Radnor, PA) by addition of a drop of ProLong Diamond antifade reagent containing DAPI (ThermoFisher Scientific, P36962). Samples were imaged with confocal laser scanning microscope Leica SP8 (Leica Microsystems Inc., Wetzlar, Germany). All images within each sample set were captured using identical instrument settings. Acquisition was performed in three sequences to minimize bleed-through artifacts. DAPI was excited at 405 nm with UV laser and detected at 415-480 nm during the first sequence. Alexa Fluor 488 was excited at 499 nm and detected at 498-600 nm during the second sequence. Alexa Fluor 647 was excited at 647 nm and detected at 667-800 nm. Image analysis was performed using Imaris 9.5.1 (Bitplane, Belfast, UK) with nuclear detection based on DAPI staining.

ELISA

Hepatitis B e antigen (HBeAg) was detected in culture media at the indicated time by electrochemiluminescence assay (MSD). The MSD assay was performed according to the

manufacturer's instructions (Meso Scale Diagnostics, Rockville, MD). Briefly, cultured supernatants were inactivated with 0.5% Triton X-100 (30 minutes at 37ºC) and then transferred into plates pre-spotted with an anti-HBeAg antibody (Genway Bio, San Diego, CA). The plates were then incubated for 2 hours at room temperature with gentle shaking, followed by a wash step in PBS with 0.5% Tween. MSD Sulfate tags anti-A and anti-B (1 µg/ml each) were then added to the wells and the plates incubated for a further 2 hours at room temperature with gentle shaking, followed by another wash step in PBS with 0.5% Tween. A 2X solution of MSD T Buffer Read was then added and the plate was read on a Sector Imager 6000 plate scanner.

RT-PCR Analysis

Total cellular RNA was isolated from PHH cultured in 96-well plates using an RNeasy 96 Kit (Qiagen) following the manufacturer's instructions. Real-Time RT-PCR was performed with TaqMan1 Fast Virus 1-Step Master Mix (Life Technologies) using a QuantStudio 7 Flex Real-Time PCR System (Life Technologies) following the manufacturer's instructions. β-actin mRNA expression was used to normalize target gene expression. All oligonucleotide primer sets were manufactured by Life Technologies.

Statistical analysis

Statistical significance of log-transformed data was tested using a two-tailed, paired t-test (for two sample comparisons) or unpaired one-way ANOVA with Dunnett’s multiple comparison correction (for multiple comparisons). A value of $p<0.05$ was considered significant.

Data availability

All data are available from corresponding authors upon reasonable request.

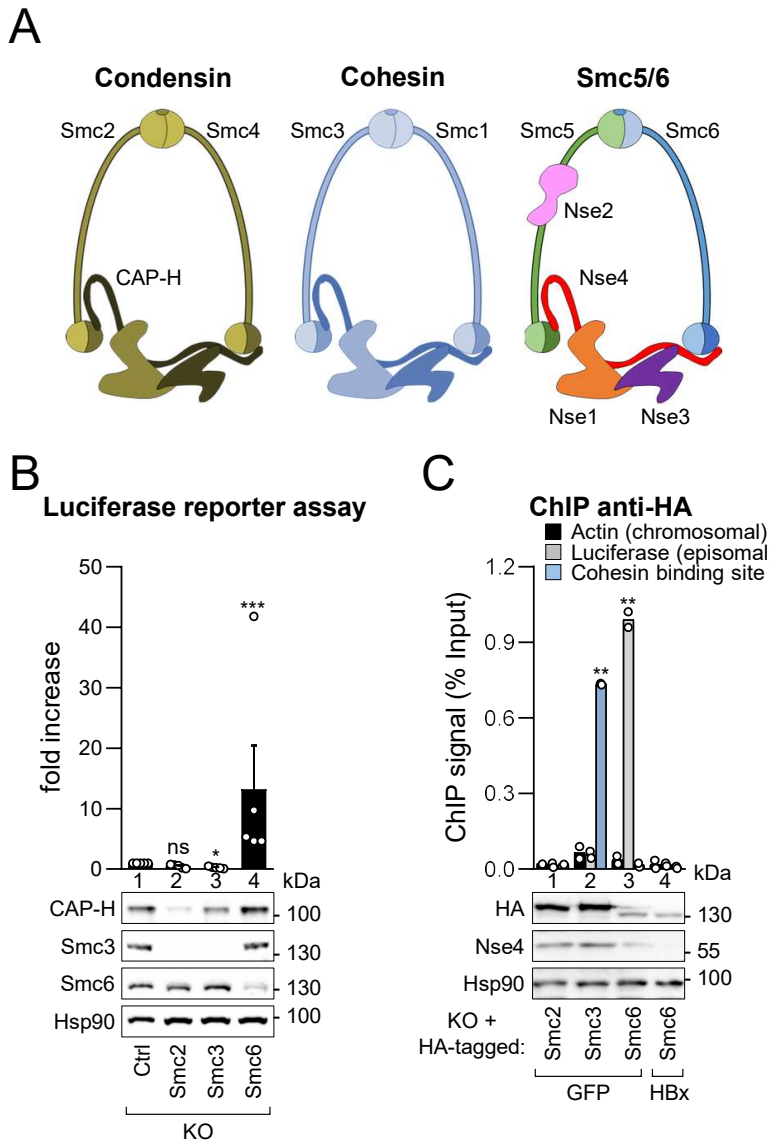
A
Condensin
Cohesin
Smc5/6
Smc2
Smc4
Smc3
Smc1
Smc5
Smc6
Nse2
CAP-H
Nse4
Nse1
Nse3
B
Luciferase reporter assay
fold increase
50
40
30
20
10
0
***
ns
*
1
2
3
4
kDa
CAP-H
Smc3
Smc6
Hsp90
100
130
130
100
Ctrl
Smc2
Smc3
Smc6
KO
C
ChIP anti-HA
Actin (chromosomal)
Luciferase (episomal)
Cohesin binding site
ChIP signal (% Input)
1.2
0.9
0.6
0.3
0.0
**
**
1
2
3
4
kDa
HA
Nse4
Hsp90
130
55
100
KO +
HA-tagged:
Smc2
Smc3
Smc6
Smc6
GFP
HBx

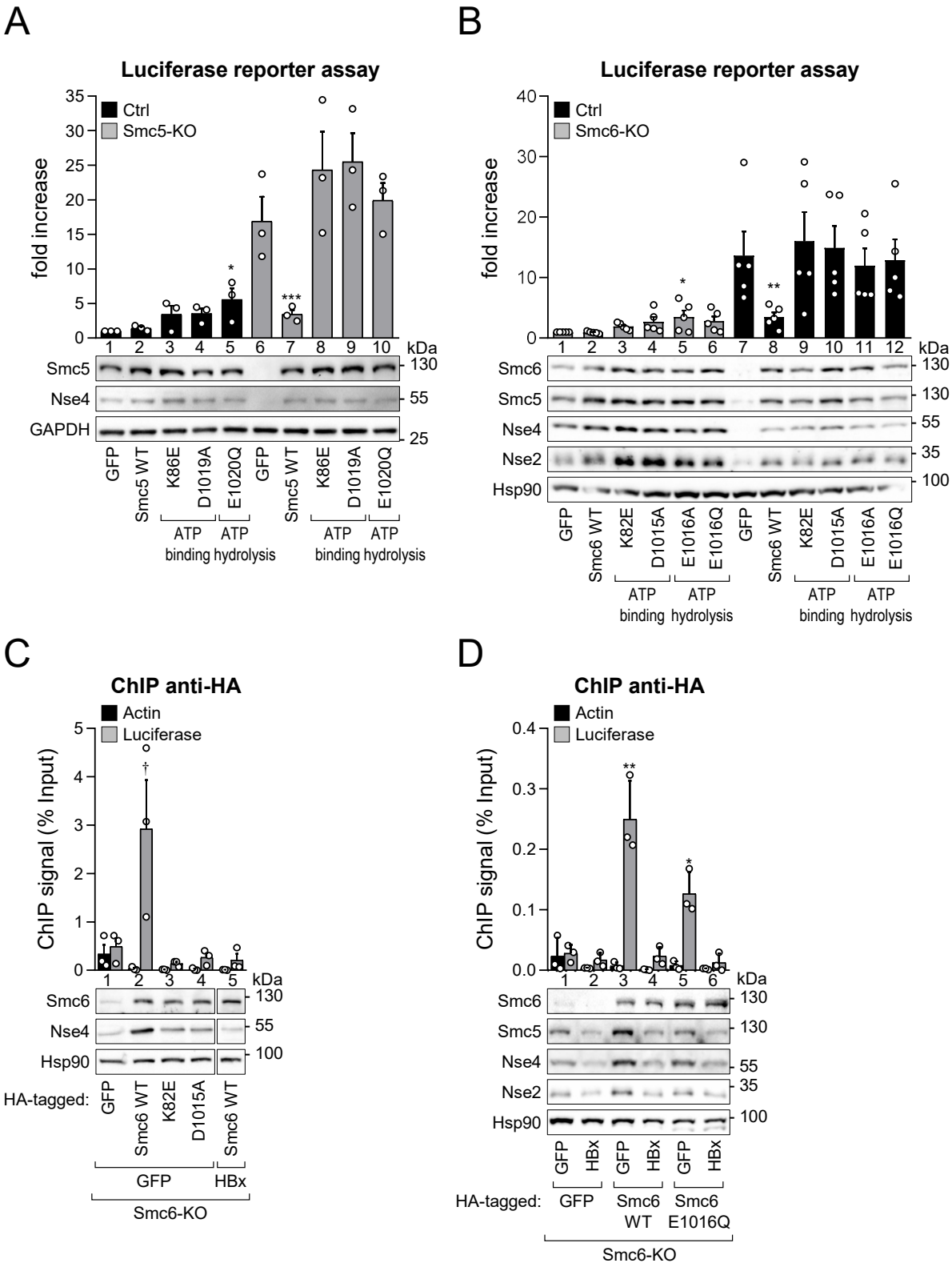
A
Luciferase reporter assay
Ctrl
Smc5-KO
fold increase
kDa
Smc5
Nse4
GAPDH
GFP
Smc5 WT
K86E
D1019A
E1020Q
ATP binding
ATP hydrolysis
B
Luciferase reporter assay
Ctrl
Smc6-KO
fold increase
Smc6
Smc5
Nse4
Nse2
Hsp90
GFP
Smc6 WT
K82E
D1015A
E1016A
E1016Q
C
ChIP anti-HA
Actin
Luciferase
ChIP signal (% Input)
HA-tagged:
GFP
Smc6 WT
K82E
D1015A
HBx
Smc6-KO
D
ChIP anti-HA
Actin
Luciferase
ChIP signal (% Input)
HA-tagged:
Smc6 WT
Smc6 E1016Q
Smc6-KO

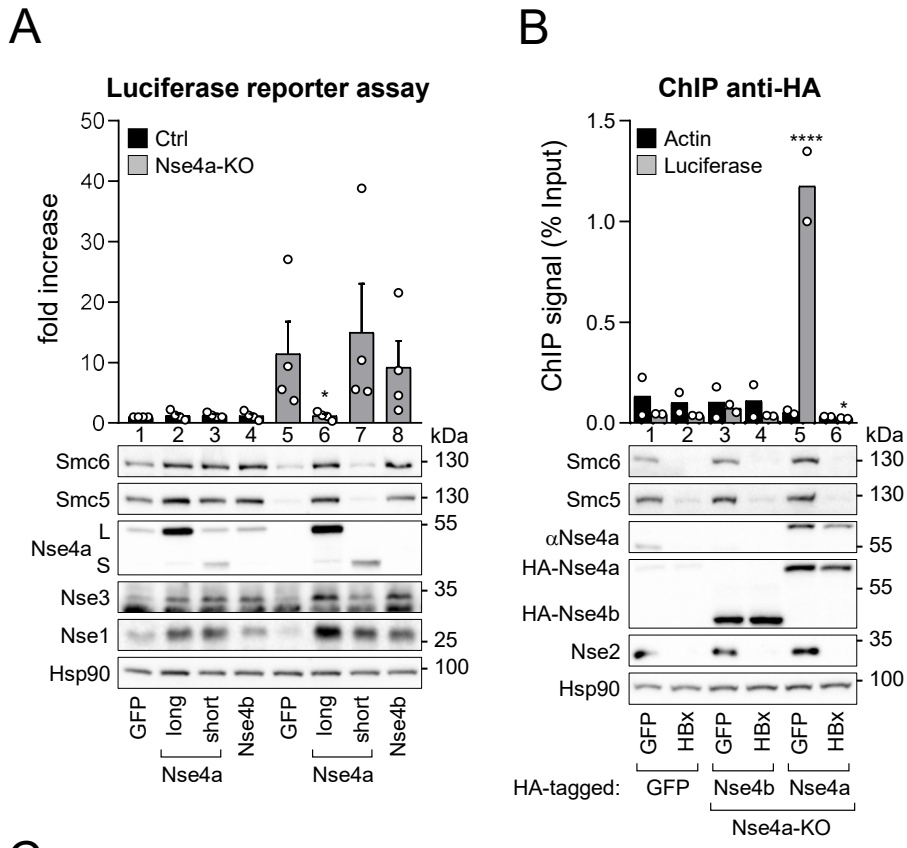
A
Luciferase reporter assay
fold increase
Ctrl
Nse4a-KO
50
40
30
20
10
0
1 2 3 4 5 6 7 8
kDa
Smc6
Smc5
Nse4a L
S
Nse3
Nse1
Hsp90
130
130
55
35
25
100
GFP
long
short
Nse4b
GFP
long
short
Nse4b
Nse4a
Nse4a
B
ChIP anti-HA
ChIP signal (% Input)
Actin
Luciferase
****
1.5
1.0
0.5
0.0
1 2 3 4 5 6
kDa
Smc6
Smc5
αNse4a
HA-Nse4a
HA-Nse4b
Nse2
Hsp90
130
130
55
55
35
100
GFP
HBx
GFP
HBx
GFP
HBx
HA-tagged:
GFP
Nse4b
Nse4a
Nse4a-KO
C
Ctrl
Nse4a-KO
Mock
GFP
Nse4a Long
Nse4a Short
Nse4b EID3

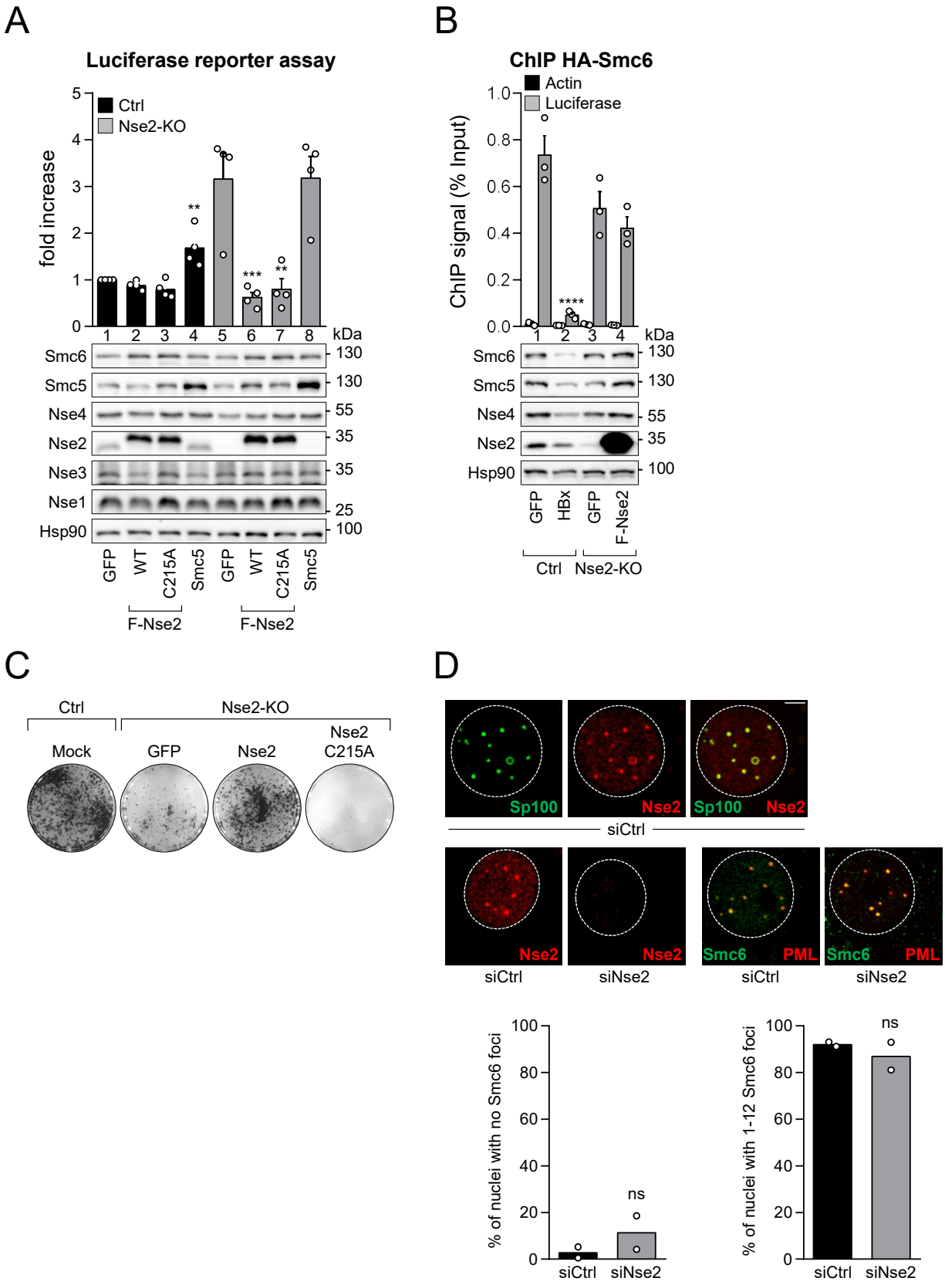
A
Luciferase reporter assay
Ctrl
Nse2-KO
fold increase
kDa
Smc6
Smc5
Nse4
Nse2
Nse3
Nse1
Hsp90
GFP
WT
C215A
Smc5
F-Nse2
B
ChIP HA-Smc6
Actin
Luciferase
ChIP signal (% Input)
GFP
HBx
F-Nse2
Ctrl
Nse2-KO
C
Ctrl
Nse2-KO
Mock
GFP
Nse2
Nse2 C215A
D
Sp100
Nse2
siCtrl
siNse2
Smc6
PML
% of nuclei with no Smc6 foci
% of nuclei with 1-12 Smc6 foci
ns

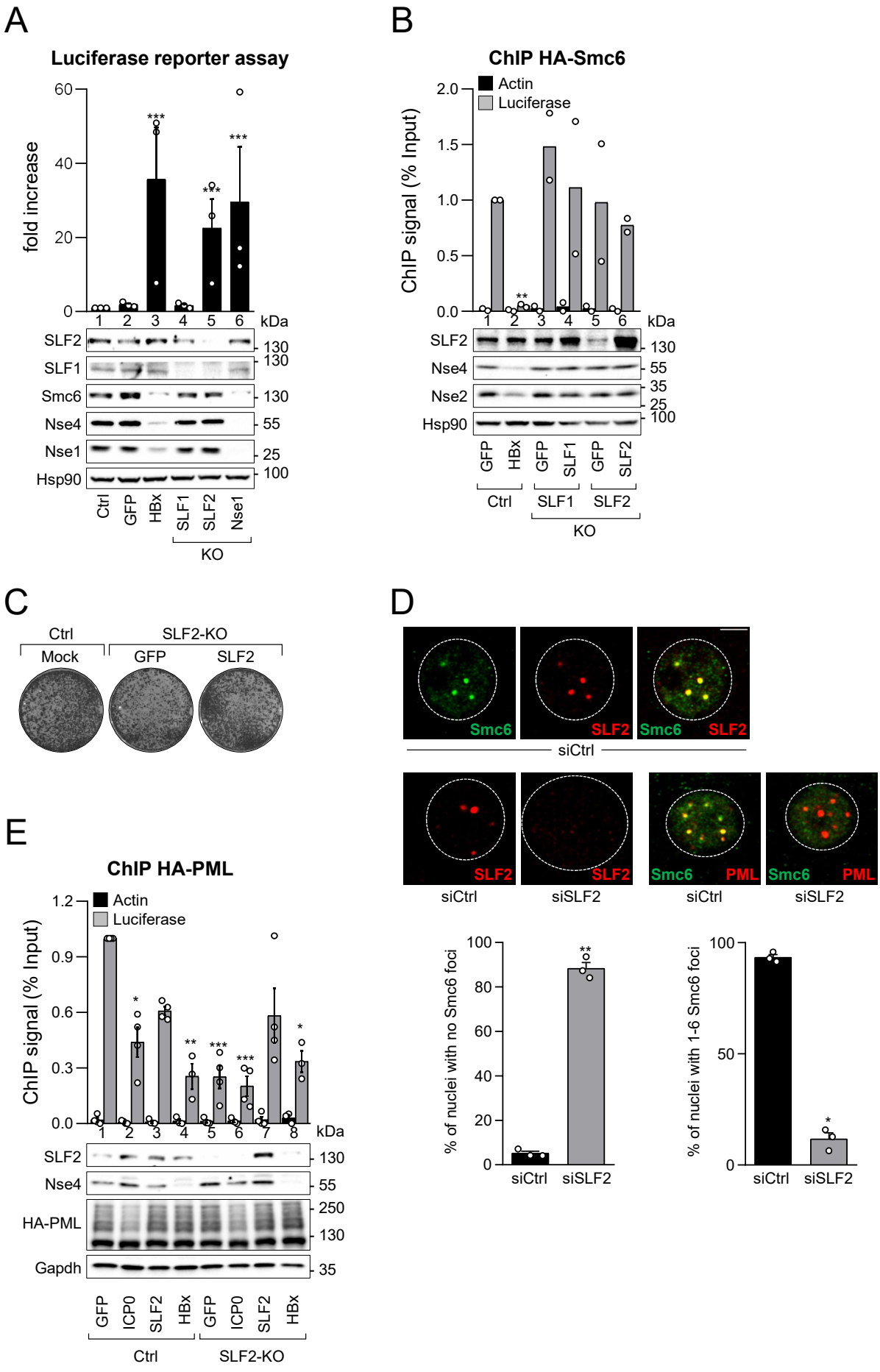
A
Luciferase reporter assay
fold increase
60
40
20
0
***
***
***
1 2 3 4 5 6
kDa
SLF2
SLF1
Smc6
Nse4
Nse1
Hsp90
130
130
130
55
25
100
Ctrl
GFP
HBx
SLF1
SLF2
Nse1
KO
B
ChIP HA-Smc6
Actin
Luciferase
ChIP signal (% Input)
2.0
1.5
1.0
0.5
0.0
**
1 2 3 4 5 6
kDa
SLF2
Nse4
Nse2
Hsp90
130
55
35
25
100
GFP
HBx
GFP
SLF1
GFP
SLF2
Ctrl
SLF1
SLF2
KO
C
Ctrl
SLF2-KO
Mock
GFP
SLF2
D
Smc6
SLF2
Smc6
SLF2
siCtrl
SLF2
SLF2
Smc6
PML
Smc6
PML
siCtrl
siSLF2
siCtrl
siSLF2
% of nuclei with no Smc6 foci
100
80
60
40
20
0
**
siCtrl
siSLF2
% of nuclei with 1-6 Smc6 foci
100
50
0
*
siCtrl
siSLF2
E
ChIP HA-PML
Actin
Luciferase
ChIP signal (% Input)
1.2
0.9
0.6
0.3
0.0
*
**
***
***
*
1 2 3 4 5 6 7 8
kDa
SLF2
Nse4
HA-PML
Gapdh
130
55
250
130
35
GFP
ICP0
SLF2
HBx
GFP
ICP0
SLF2
HBx
Ctrl
SLF2-KO

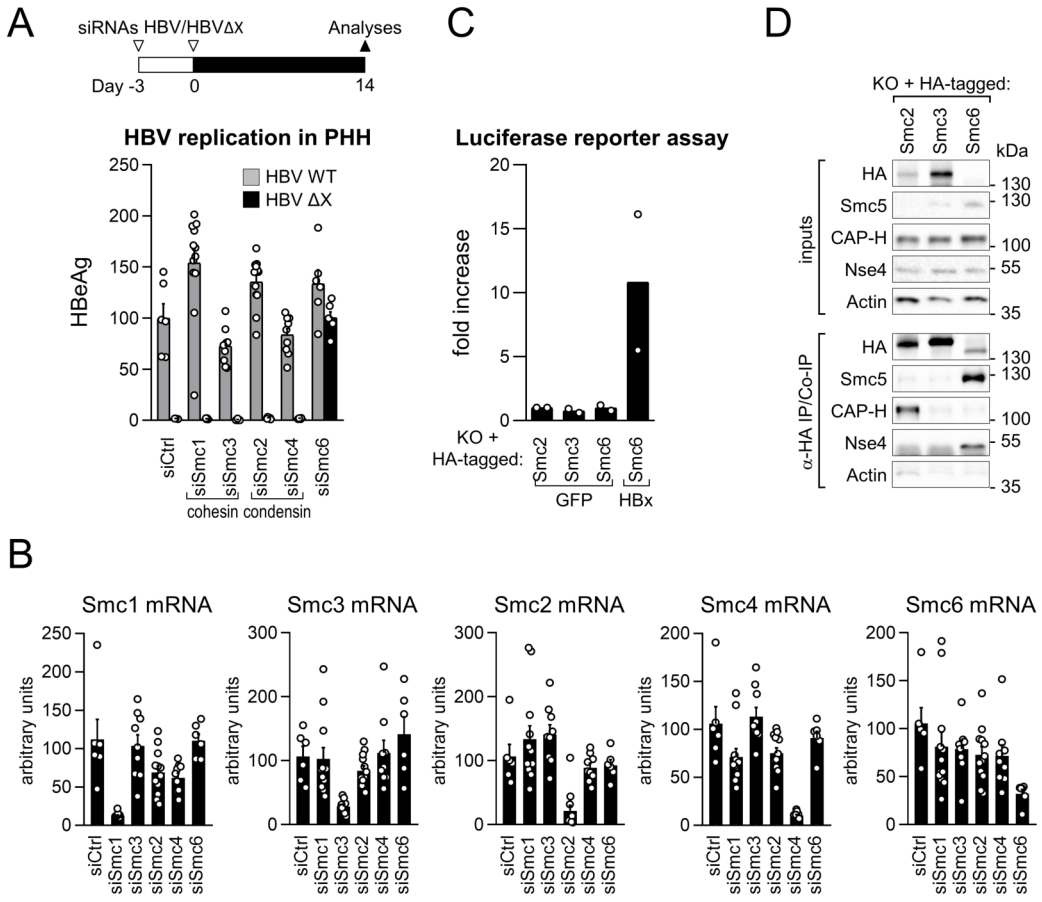

Extended Data Figure 1. Smc5/6 is the only SMC complex to silence expression of the episomal HBV genome. Related to Figure 1.

a, PHH were transfected with a non-targeting control siRNA (siCtrl) or with siRNA targeting the indicated Smc subunits. Cells were then incubated for 3 days and infected with wild-type (WT) or an HBx-deficient (ΔX) HBV. HBeAg secretion, a marker for HBV gene expression, was measured 14 days later. HBeAg levels are expressed as a percentage of those in control cells infected with HBV(WT) (grey bars) or in siSmc6-treated cells infected with HBV(ΔX) (black bars). Data are means ± SEM of three independent experiments with samples from one PHH donor. The schematic diagram summarizing the design of the study is shown at the top.

b, The mRNA levels of the indicated Smc proteins in the samples analyzed in **a** were determined by real-time RT–PCR and normalized to β-actin. Values are expressed as a percentage of those in control cells (siCtrl). Data are means ± SEM of three independent experiments with one PHH donor.

c, Luciferase assay for the ChIP experiment presented in Fig, 1c. Data are means ± SEM of 2 independent experiments.

d, HA-Smc2 assembles into a condensin complex. Whole extracts prepared from HepG2 cells expressing the indicated HA-tagged SMC protein in a CRISPR/Cas9 knockout background were immunoprecipitated with anti-HA antibodies. The amounts recovered and the presence of Smc5, CAP-H and Nse4 in the eluates were assessed by Western blotting. CAP-H and Nse4 are the kleisin subunits of, respectively, condensin (Smc2) and the Smc5/6 complex. See Fig. 1a. Actin serves as a negative control. The experiment was repeated twice independently with similar results.

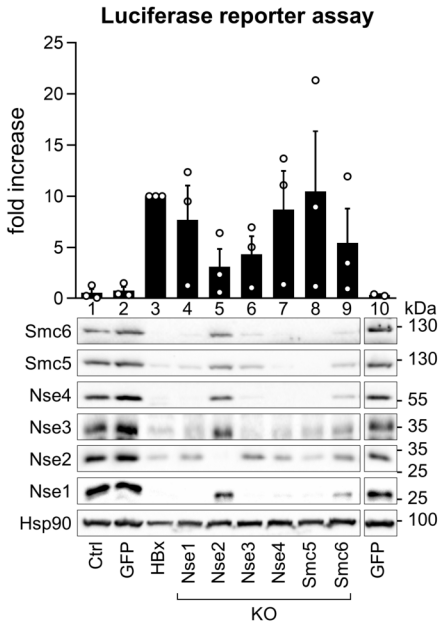

Extended Data Figure 2. Effect of single-subunit depletion on Smc5/6 complex integrity and restriction activity.

HepG2 cells were transduced with lentiviral constructs expressing Cas9 alone (Ctrl) or Cas9 together with sgRNA targeting the indicated Smc5/6 subunits, or with lentiviruses encoding GFP or GFP-HBx, as indicated. After selection, cells were transfected with a luciferase reporter plasmid. Luciferase assay and Western blot analysis were performed 5 days later. Hsp90 serves as a loading control. Unessential lanes were removed from the original blot images. Luciferase activity is relative to that measured in cells expressing HBx, which was set to 10. Data are means ± SEM of 3 independent experiments.

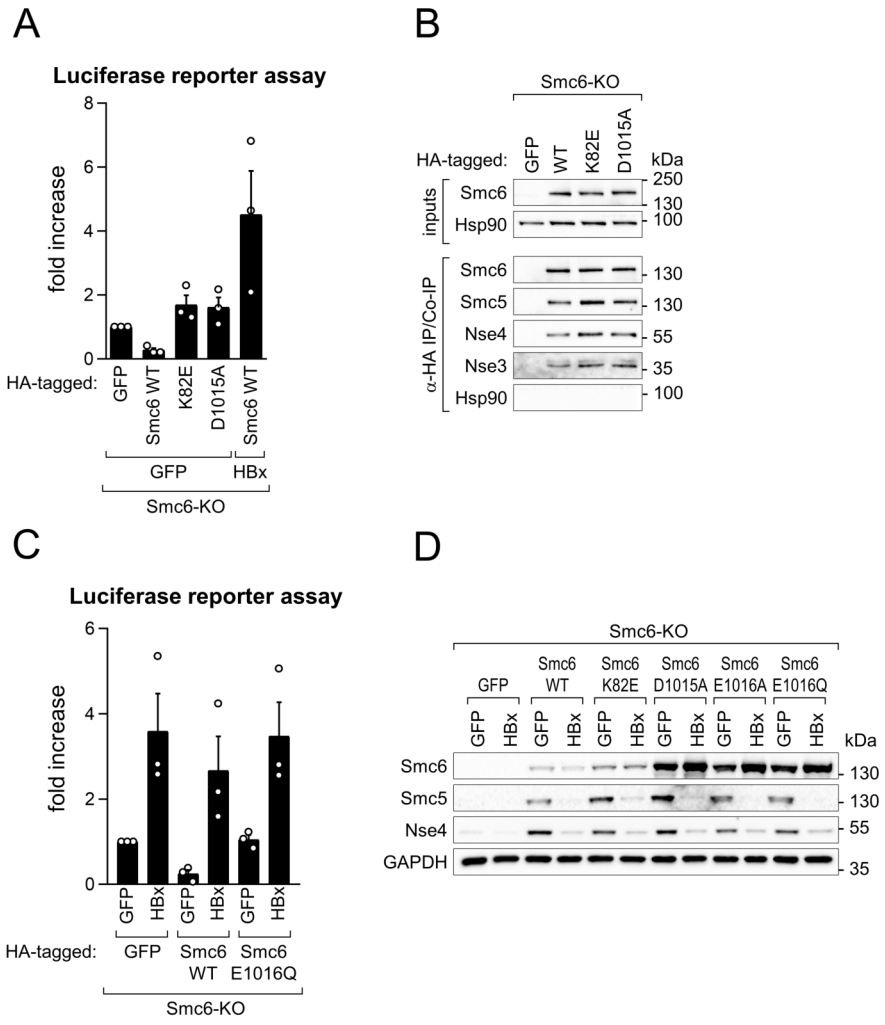

Extended Data Figure 3. Involvement of Smc5 and Smc6 ATP binding and hydrolysis in Smc5/6 episomal DNA binding and restriction, and degradation by HBx. Related to Figure 2.

a, Luciferase assay for the ChIP experiment presented in Fig. 2c. Data are means ± SEM of 3 independent experiments.

b, Smc6 ATP binding mutants normally assemble into Smc5/6 complexes. Whole extracts prepared from HepG2 cells depleted of Smc6 and expressing HA-GFP or the indicated HA-tagged SMC protein were immunoprecipitated with anti-HA antibodies. The amounts recovered and the presence of other Smc5/6 subunits in the eluates were assessed by Western blotting. Hsp90 serves as a negative control. The experiment was repeated twice independently with similar results.

c, Luciferase assay for the ChIP experiment presented in Fig, 2d. Data are means ± SEM of 3 independent experiments.

d, HepG2 cells depleted of Smc6 and expressing GFP or the indicated wild-type or mutant Smc6 proteins from lentiviral vectors exactly as in Fig. 2b were also transduced with GFP or GFP-HBx. Western blot analysis was performed as before. GAPDH serves as a loading control. The experiment was repeated thrice independently with similar results.

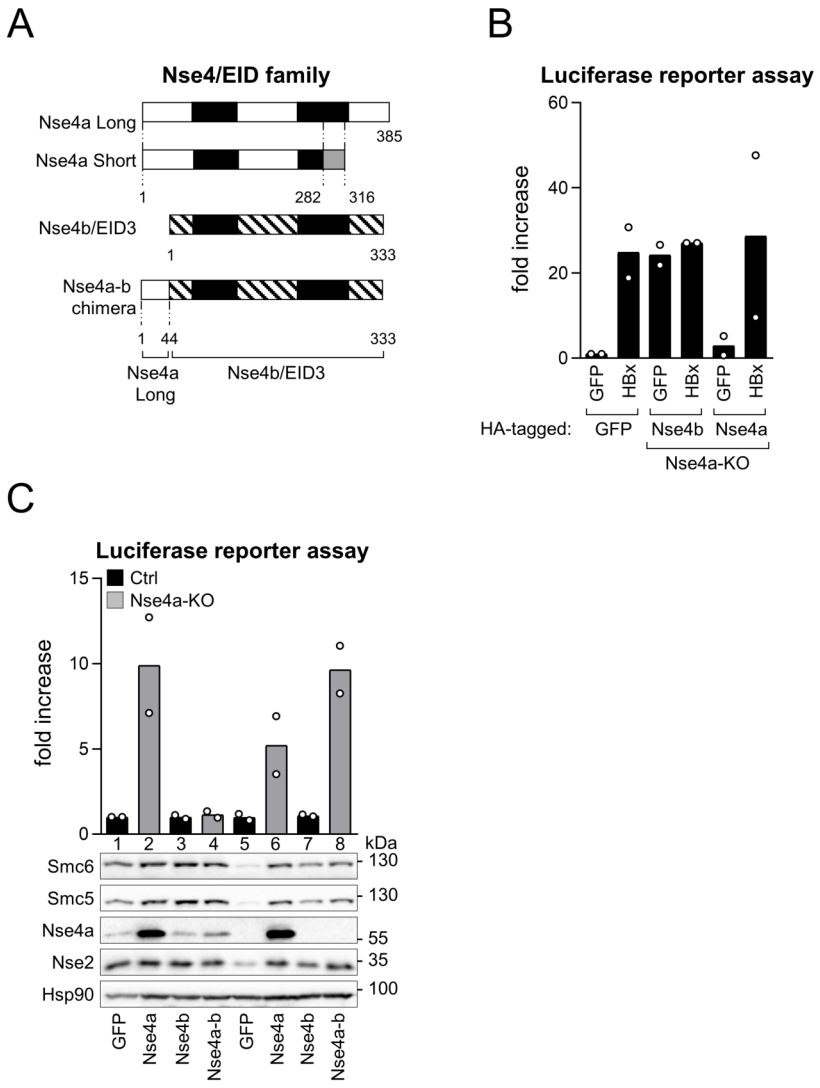

Extended Data Figure 4. Nse4a performs an essential function in Smc5/6 restriction for which Nse4b cannot substitute. Related to Figure 3.

a, Schematic diagram of Nse4a (long), the shorter isoform of Nse4a, Nse4b and the Nse4b variant bearing the N-terminal region unique to Nse4a. White boxes indicate Nse4a sequences and the region of the short Nse4a protein common to both splicing isoforms. Hatched boxes indicate regions of Nse4b showing homology to Nse4a. The grey box indicates a region with no homology. Highlighted in black are the highly conserved N-terminal and C-terminal kleisin domains that have the potential to form helix-turn-helix and winged-helix motifs and are involved in Nse4 interaction with Smc6 and Smc5, respectively (Palecek et al., 2006; Vondrova et al., 2020).

b, Luciferase assay for the ChIP experiment presented in Fig. 3b. Data are means ± SEM of 2 independent experiments.

c, Same experiment as in Fig. 3a but including an Nse4b chimeric protein carrying the N-terminal region unique to Nse4a (Nse4a-b; see panel **a**). Expression of Nse4b and Nse4a-b was inferred from their stabilization effect on the other Smc5/6 subunits (lane 8). Data are means ± SEM of 2 independent experiments.

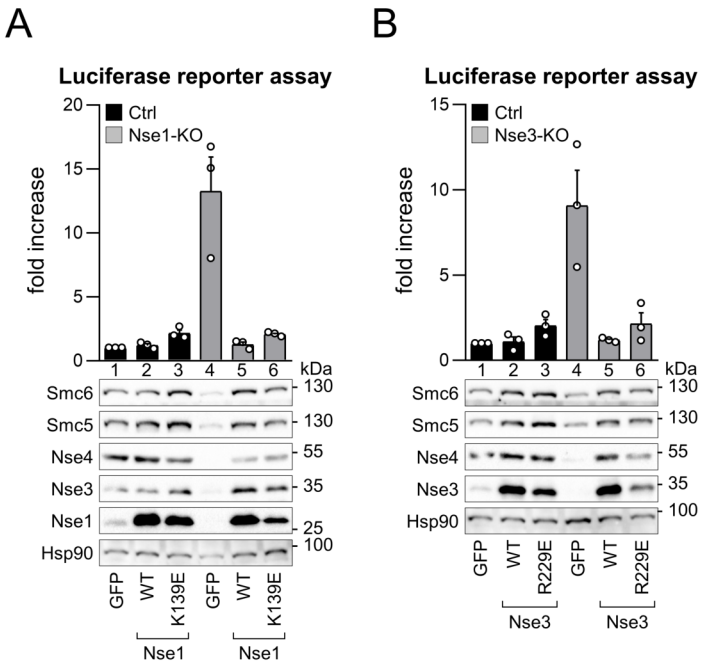

Extended Data Figure 5. Nse1 and Nse3 DNA-binding mutants are functional in vivo.

a,b, Control HepG2 cells (black bars) and cells depleted of Nse1 (**a**) or Nse3 (**b**; grey bars) were transfected with a luciferase reporter plasmid and shortly after transduced with GFP or the corresponding wild-type or DNA-binding mutant protein as indicated (Zabrady et al., 2016). Luciferase assay and Western blot analysis were as before. Data are means ± SEM of 3 independent experiments.

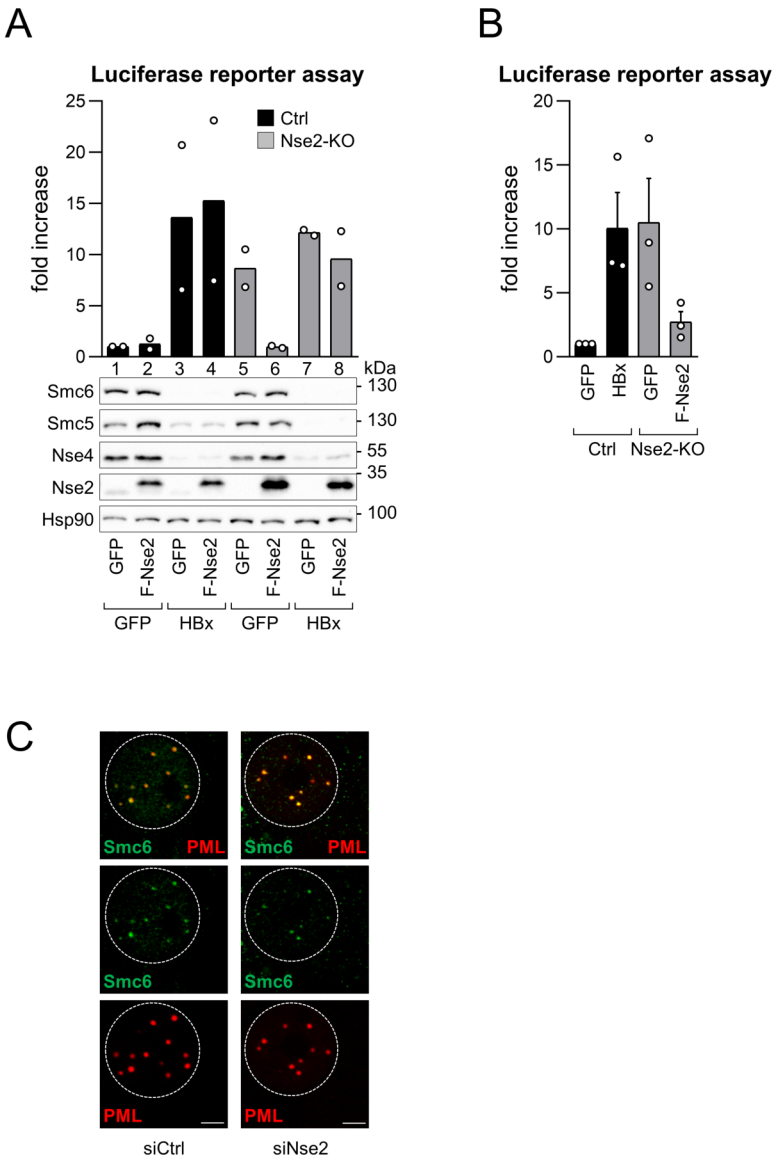

Extended Data Figure 6. HBx triggers Smc5/6 degradation in the absence of Nse2. Related to Figure 4.

a, Control HepG2 cells (black bars) and cells depleted of Nse2 (grey bars) were transfected with a reporter gene and transduced with GFP or Flag-tagged Nse2 (F-Nse2). Cells were then split and further transduced with GFP or GFP-HBx. Luciferase assay and Western blot analysis were as before. Data are expressed as mean ± SEM of 2 independent experiments.

b, Luciferase assay for the ChIP experiment presented in Fig. 4b. Data are expressed as mean ± SEM of 3 independent experiments.

c, Single channel confocal images of middle right panels merged images presented in Fig. 4d.

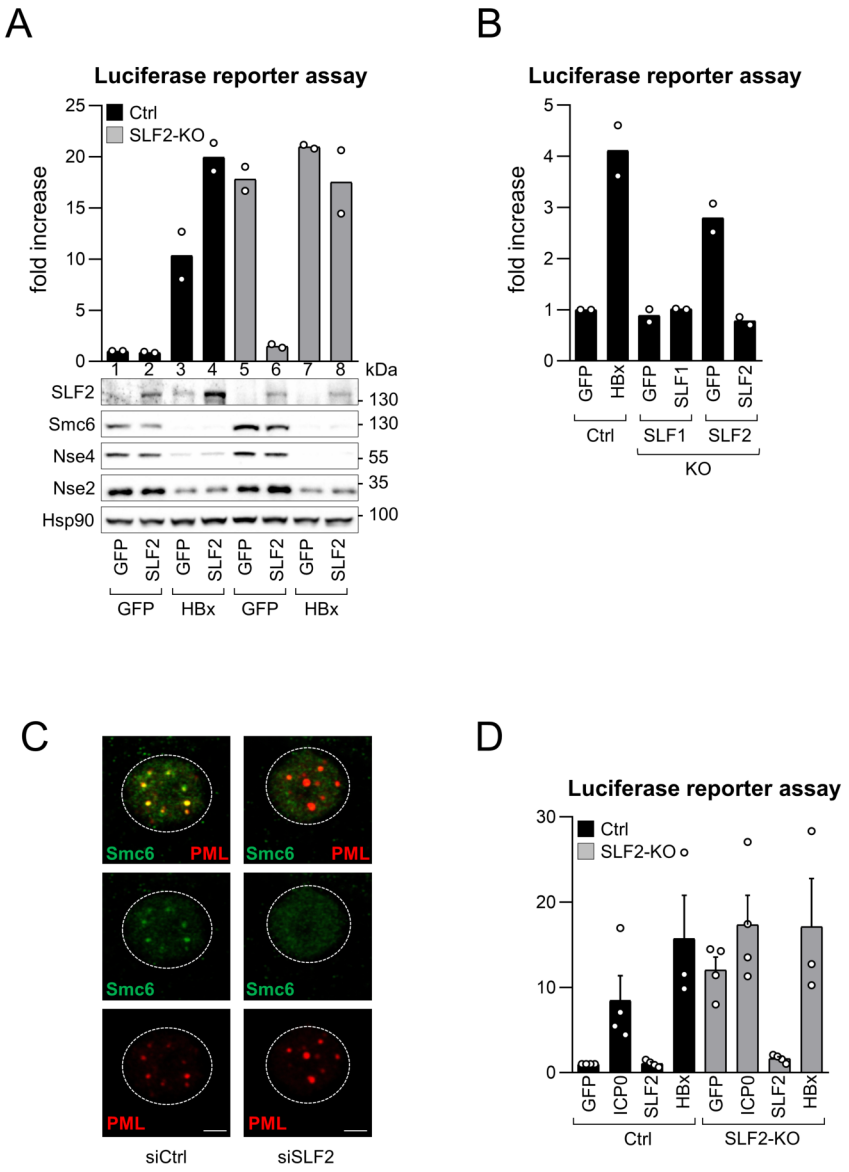

Extended Data Figure 7. HBx triggers Smc5/6 degradation in the absence of SLF2. Related to Figure 5.

a, Control HepG2 cells (black bars) and cells depleted of SLF2 (grey bars) were transfected with a reporter gene and shortly after transduced with GFP, GFP-HBx and/or SLF2 in the indicated combinations. Luciferase assay and Western blot analysis were performed as before. Data are expressed as mean ± SEM of 2 independent experiments.

b, Luciferase assay for the ChIP experiment presented in Fig. 5b. Data are means ± SEM of 2 independent experiments.

c, Single channel confocal images of middle right panels merged images presented in Fig. 5d.

d, Luciferase assay for the ChIP experiment presented in Fig. 5e. Data are means ± SEM of 4 independent experiments.